

# TinyEmo: Scaling down Emotional Reasoning via Metric Projection

Cristian Gutierrez

## Abstract

This paper introduces TinyEmo, a family of small multi-modal language models for emotional reasoning and classification. Our approach features: (1) a synthetic emotional instruct dataset for both pre-training and fine-tuning stages, (2) a Metric Projector that delegates classification from the language model allowing for more efficient training and inference, (3) a multi-modal large language model (MM-LLM) for emotional reasoning, and (4) a semi-automated framework for bias detection. TinyEmo is able to perform emotion classification and emotional reasoning, all while using substantially fewer parameters than comparable models. This efficiency allows us to freely incorporate more diverse emotional datasets, enabling strong performance on classification tasks, with our smallest model (700M parameters) outperforming larger state-of-the-art models based on general-purpose MM-LLMs with over 7B parameters. Additionally, the Metric Projector allows for interpretability and indirect bias detection in large models without additional training, offering an approach to understand and improve AI systems. We release code, models, and dataset at <https://github.com/ggcr/TinyEmo>

## Index Terms

Affective Computing, Visual Sentiment Analysis, Multi-modal LLM, Visual Question Answering, Visual Instruction Tuning.

## I. INTRODUCTION

Visual Sentiment Analysis is the ability to automatically recognize and interpret emotions from visual content. Notice that “sentiment” and “emotion” are used interchangeably, though they are distinct concepts [1]. The name of the field reflects its origins in text-based Sentiment Analysis from NLP, where sentiments (opinion-based) are more common. In visual content, however, raw emotions are more prominent, leading to a focus on emotion recognition despite retaining the term “sentiment”. The field draws upon psychological emotional representation models, which have been developed to categorize emotions into categorical and dimensional types. Categorical Emotion States (CES), like Ekman’s 6 basic emotions [2] and Parrott’s hierarchical categorization of 25 emotions [3], treat emotions as distinct categories. In contrast, Dimensional Emotion Space (DES), such as the Valence-Arousal (VA) space [4], represent emotions along continuous dimensions. Our work focuses on CES models, posing Visual Sentiment Analysis as a discrete-label classification problem. This ability to bridge the gap between visual data and emotional understanding enables a range of practical applications that can benefit from it [5] to help assess mental health conditions and improve human-computer interactions.

In recent years, research in multi-modal large language models (MM-LLMs) for image-text understanding has exploded [6]. Open-source models like Instruct-BLIP [7] and LLaVA [8] popularized “visual instruction tuning” by combining instruction tuning from NLP and visual understanding tasks. These MM-LLMs combine a Vision Encoder (ViT) [9], a cross-modal projector and an LLM backbone. While previous work in Visual Sentiment Analysis has primarily focused on emotion classification, EmoVIT [10] was the first to leverage a MM-LLM to provide both classification and reasoning capabilities, explaining the emotional content of an image, beyond just a label. This approach has demonstrated promising results using a general-purpose MM-LLM architecture. However, it has also proven to be computationally intensive for down-stream tasks. To the best of our knowledge, little work has been done in exploring the role of the projector specifically for emotional downstream tasks. There remains a significant gap for research in the adaptation of these general architectures for specific downstream tasks, particularly in the domain of emotion analysis. In our work, we intend to make models smaller and adjust parts to work better with fewer parameters, specifically targeting emotional downstream tasks.

Zhao *et al.* [11] identifies three main challenges in Visual Sentiment Analysis: (1) the affective gap, which represents the discrepancy between the predicted and the actual emotional response; (2) perception subjectivity, where different viewers may have varying emotional reactions on the same image; and (3) label noise and absence, reflecting the difficulty in obtaining large-scale, and reliable, emotional labels. To address the lack of datasets for the down-stream task of emotional reasoning we introduce a Emotional Visual Instruct dataset, designed for both pre-training and fine-tuning stages. This dataset, combined with the extra projector trained with metric learning, allows for better zero-shot performance and easier exploration

Author: Cristian Gutierrez, cgutierrezgome@uoc.edu

Advisor 1: Cristina Bustos, Artificial Intelligence for Human Well-being (AIWELL), Universitat Oberta de Catalunya

Advisor 2: Agata Lapedriza, Artificial Intelligence for Human Well-being (AIWELL), Universitat Oberta de Catalunya

Thesis dissertation submitted: September 2024

of textual and visual hidden representations. We propose a system capable to assess all these challenges for which our model must (1) incorporate context into the decision-making process, (2) contemplate multi-label emotion classification, and (3) unsupervised/weakly supervised learning and/or few/zero-shot learning to manage the lack of labeled datasets and improve knowledge transfer across multiple emotional taxonomies and domains. Providing a way to evaluate models over any emotional taxonomy and benchmarks available through different domains simultaneously.

Our work with TinyEmo introduces an extra projector that detaches the classification task from the Language Model (LLM), allowing the LLM to focus solely on reasoning. This decision is motivated by recent findings [12], [13] that highlight limitations in fine-grained classification tasks for MM-LLMs. We demonstrate that this split strategy optimizes training and leads to better performance, as it allows for having two independent training objectives on different core components of our architecture. Furthermore, this approach allows us to overcome computational limitations faced by previous models like EmoVIT [10], which could only train on 50% of its dataset due to resource constraints. The convenient positioning of the projector between the Vision Encoder (ViT) and the LLM allows us to explore the relationships between these pre-trained core components of our architecture and the incorporation of more diverse datasets. By investigating both textual and visual embeddings, we aim to uncover hidden learned representations and detect biases in larger models on visual emotional content.

**Our contributions.** Our contributions are summarized as follows:

- We create an Emotional Visual Instruct dataset designed for both pre-training and fine-tuning stages, combining abundant synthetic data generated by a smaller model with high-quality samples from a larger model. This dataset addresses the challenges of limited data on emotional reasoning tasks.
- We introduce an extra metric-learning cross-modal projector that handles emotion classification, allowing the LLM to focus solely on reasoning. We demonstrate that this architecture achieves better performance with less computational overhead for emotion related downstream tasks.
- We build a multi-modal large language model (MM-LLM) specifically designed for the emotional reasoning task, incorporating the projector for the classification detachment.
- We propose a semi-automated framework using the projector to detect biases in larger models with no additional training, offering a new approach to understand and improve multi-modal systems.

## II. STATE OF THE ART

**Datasets.** Emotions are present in a quite variety of datasets, the most important for this present work are the Visual Sentiment Datasets which are annotated with emotion-related labels. Panda *et al.* [14] presented two training datasets; WEBEmo includes 268k stock photos across 25 emotion categories using Parrott's [3] hierarchical model, and Emotion6 [14] that is smaller with 8,350 images and follows Ekman's [2] six emotions. They then present UnbiasedEmo [14], an evaluation dataset addressed to mitigate biases from diverse data sources. EmoSet [15] is a more recent dataset that contains a total of 118k & 3M images annotated with the sentiment label and additional image annotations such as brightness, scene, facial expression, among others. Other notable datasets in no particular order are Flickr and Instagram [16], FI [17], ArtPhoto [18], Abstract [18], IAPS [19] and OxfordTVG-HIC [20] which is intended for humorous purposes. Other datasets we distinguish from are Visual Emotion Recognition Datasets, which also include specific ROI boxes to highlight areas of interest within the images that are crucial for emotion recognition tasks; notable work in this field include EMOTIC [21], [22] as the first benchmark to support emotion recognition in real-world contexts, and EmotionROI [23]. Finally, the interest of emotions has been growing on pose generation, from which we highlight EMoG [24] that provides 3D gesture data with emotional cues. Additional work of particular interest for this present work include Art-Emis [25] and Affective Explanations [26] datasets, they employ images from popular datasets (i.e. WikiArt dataset [25], or MS-COCO [27]) with the sentiment label and a manually annotated affective explanation for what the viewer felt watching that particular painting/image.

Different datasets adopt varied taxonomies, i.e. ways of representing emotions, and they do so because there is not an universal agreement on how to categorize them. The choice of taxonomy is mostly motivated by the own dataset's authors methodology, goals and intended approach, allowing for this to be based on each-other needs. As an example, WEBEmo authors decided to pursue a three-level emotion hierarchy based on Parrott taxonomy to alleviate the search engine bias by diversifying the image search and to structure their proposed approach based on curriculum learning [28]. This method mirrors human cognitive system by starting with simpler tasks and progressively introducing more complex ones, in this case, starting from binary categorization of *positive* or *negative* emotions before advancing to gradually more populated taxonomies. Interestingly, dataset selection can also be driven by additional features of interest. For instance, EmoVIT [10] authors chose EmoSet as their training dataset mainly because of the inclusion of additional visual attributes, such as brightness, scene type or facial expression, among others. This choice suited better their needs to investigate whether this supplementary information could be beneficial for emotion classification and reasoning.

**Visual encoding.** Vision Transformers (ViTs) are a special type of transformers, intended for visual content, with an encoder only architecture. It treats images not as grids of pixels but rather as sequences of flattened patches, which aligns with the

intended purpose of transformers [29], originally built to handle sequences of text. Image patches are linearly projected using a trainable matrix into embeddings to match the dimensionality  $d$  used in the transformer, akin to generating word embeddings in NLP. ViT introduces a special `CLS` token [30], this token is appended to the sequence of embedded patches (at the beginning, typically) and is used as an aggregated representation for the entire image. The visual encoder role is to transform the input image patches and their positional encodings into a series of embeddings that capture both local and global relationships within the image. McKinzie *et al.* [31] emphasize the importance of the Vision Encoder (ViT) in multi-modal language models, noting that image resolution plays a critical role; higher resolutions generally result in more visual tokens processed by the system, depending on the encoder's patch size. CLIP [32], was one of the first models to scale and leverage a large pre-training on image-text pairs with metric learning. Thus, making it ideal for transfer learning and zero-shot purposes. Recent work has been put onto making CLIP more efficient, both at train time and inference time [33]. There is also more ambitious on-going work on leveraging vision-only encoders, that do not depend on text [34], useful for exclusively vision related tasks.

On Visual Sentiment Analysis, Bustos *et al.* [35] took note of CLIP capabilities for fine-grained classification and proposed CLIP-E, an extension that adds non-linear fully-connected layers atop the frozen CLIP vision encoder to capture more useful features for the downstream task of fine-grained emotion classification, employing both traditional cross-entropy and metric learning approaches. Demonstrating a significant reduction in training parameters and computational requirements while maintaining the versatility of having a pre-trained model for quick adaptation to new downstream tasks.

**Visual-Instruction Tuning.** The integration of instruction-tuning in large language models (LLMs) addresses limitations in zero-shot performance. Wei *et al.* [36] showcased how early LLMs performed well on few-shot tasks but struggled with zero-shot tasks due to the lack of similar exemplars. Instruction-tuning emerged as a method to improve LLMs ability to handle diverse zero-shot tasks by providing instruction-following prompts. In parallel, Visual Question-Answering (VQA) enabled models to perform visual understanding, creating an ideal synergy for training multi-modal LLMs that took nobody by surprise [7], [8], [37], [38]. By incorporating instruction-tuning from NLP into computer vision, we enhance both vision comprehension and zero-shot capabilities at a moderate cost [39]. This approach, termed “visual instruction tuning,” forms the foundation of our proposed dataset and is the core idea behind Multi-Modal Large Language Models (MM-LLMs).

MM-LLMs follow a structured architecture [6] by employing a ViT as the Vision Encoder to map images into text tokens, followed by a Projector—either with Linear fully-connected layers, Multi-Layer Perceptron (MLP) or attention mechanisms [7]—to align these features into the LLM’s feature space, culminating in an LLM Backbone which is the driving force for cognitive tasks. The training procedure was coined by pioneer work such as BLIP-2 [40] or LLaVA [8], [38], and is generally focused first on aligning the Projector on image-text pairs, followed by fine-tuning the pre-trained MM-LLM on instruction-formatted datasets, such as Visual Question-Answer (VQA) tasks [8]. More recent work has been put on the Projector, such as HoneyBee’s CAbstract [41] projector by employing ResNet [42] convolutional blocks to maintain local-visual features; or the Querying-Transformer (Q-former) [40] that use learnable vectors as queries and encoded features as keys, to refine the visual features extracted even more. Recently though, the highlight has been put onto MM-LLMs facing limitations on fine-grained object classification. Geigle *et al.* [13] evaluate MM-LLMs on a set of diverse fine-grained object classification datasets, with tasks like identifying very specific dog breeds from the Oxford-Pets dataset. Their findings reveal that even though objects are being miss-classified, the subsequent reasoning about the object is correct, thus placing the blame onto the discrete classification process itself. They primarily attribute this to differences in training data scalability. While Vision Transformers (ViTs) are trained on vast datasets on vision-only tasks, MM-LLMs are generally trained on less data with an added textual modality. This suggests that the features needed to correctly classify fine-grained objects are indeed encoded in the latent space, but LLMs are not yet able to effectively decode this information. As a result, MM-LLMs are currently missing out on fine-grained visual understanding tasks.

On Visual Sentiment Analysis, Xie *et al.* presents EmoVIT [10], one of the first alignments to leverage both Vision Encoder and LLMs cognitive abilities on the downstream task of emotion classification and reasoning by implementing a GPT-assisted pipeline for generating emotion visual instruction data, which has proven to be effective for zero-shot generalization [7], [8], [40]. Using the LAVIS library [7], [43] and the EmoSet dataset [15], they incorporate image attributes and emotion-specific instructions to enhance performance. Similarly as MM-LLMs II, they leverage a frozen Vision Encoder and a frozen LLM, and train a Q-Former [40] Projector that also encodes their emotional instruction data.

**Distillation.** The recent launch of Llama 3.1 405B as the largest open-source large language model to date, trained on over 15 trillion tokens, has sparked significant debate about the term “model distillation”. This term was mentioned multiple times in the inaugural blog post [44] by Meta, leading to discussions about its meaning and implications.

The concept of “model distillation” is a reminiscence of the machine learning concept known as “knowledge distillation,” [45] a series of continual learning methods involving training a smaller student network using a larger pre-trained network known as teacher. In traditional knowledge distillation, instead of using a regular cross-entropy loss objective, the goal is to have the smaller model approximate the underlying distribution of the master’s outputs at logit level. This objective reformulation has been proved to produce stronger student networks rather if they had been trained on regular cross-entropy objective. Hinton *et*

*al.* later described this as the student learning from the master’s “dark knowledge” [46]. However, this approach was designed for machine learning models that optimize over probability distributions, hence often trained for classification tasks over a set of fixed classes, and, with the introduction of LSTMs and LLMs featuring auto-regressive architectures and variable-length sequences, rather than the fixed-length of outputs, traditional KD had to be adapted. Two main approaches were proposed [47] either using token-level knowledge distillation over the fixed vocabulary set defined by the tokenizer or Sequence-level knowledge distillation over the fixed set of high likelihood sequences generated by the master.

Meta’s Llama 3.1 405B report [48] only mentions distillation as a method used in smaller models, citing the original Phi [49] as an example. However, the Phi team approach primarily involved using GPT-3.5 and GPT-4 to annotate a small subset of code datasets and generate synthetic content. There is no explicit mention of performing knowledge distillation at logit level in their methodology. Thus, seems uncertain they used neither token-level nor sequence-level distillation during training. We strongly believe that it is crucial to distinguish true knowledge distillation from related techniques: training on synthetic data generated by larger models, as in the case of Phi, or our approach of using a MM-LLM to generate visual instructions for training, do not qualify as distillation.

**Interpretability.** The integration of vision encoders and a projectors into multi-modal Large Language Models (MM-LLMs) has advanced their capabilities by enabling the system to understand both textual and visual modalities. The addition of these core components – the vision encoder and the language model – aligned through a cross-modal projector, each trained on its own data with different objectives, has further intensified the “black-box” [50] nature of these models. While each component has a clear role, and they interact in concert, this complexity has made the decision-making process more challenging to trace back. This paired with the new levels of unprecedented scale in models and datasets, has favoured ad-hoc interpretability techniques to be more prominent, particularly those aimed at global analysis [51] such as circuit analysis [52] and mechanistic interpretability [53]. These techniques offer post-training insights in a controllable yet massive environment.

Large Language Models (LLMs) directly assessing user-input queries provides significant benefits in explainability, offering self-insights into obscure behaviours and data patterns that otherwise we would not have access to [54]. However, these self-generated reports may be prone to hallucination [55] and subject to a speculative, yet-to-be-confirmed, consciousness limited by their context length [56]. We believe the role of individual units [57] remains a powerful way to localize activation patterns [58] that can serve as a potential measurement of internal in-depth model behaviour. Recent efforts to automate and recognize biases at scale has been put on by Shaham *et al.* with MAIA, the first multimodal agent equipped with tools for interpreting deep networks [59].

### III. METHOD

In this section we present the methodology for developing TinyEmo, a family of small multi-modal large language models (MM-LLMs) designed for emotional reasoning and classification. Our approach consists of three main contributions, that we detail in the following manner:

In Section **III-A** we introduce our Emotional Visual Instruct Dataset. This dataset is specifically tailored for emotional reasoning, and it consists of a pre-training dataset and a fine-tuning dataset. The pre-training dataset goal is to give our text-only LLMs visual capabilities, it is built upon WEBEmo dataset and we use Bunny 3B [60] to generate visual understanding tasks in a Question-Answering format. The fine-tuning dataset goal is to build on top of the already learned visual knowledge and tune it to perform Emotional Reasoning on images, this dataset is derived from the existing pre-training data, by posing the question as an instruction and the Sentiment Answer as the target answer. In Figure 1 we illustrate the creation of the dataset with a pre-training and a fine-tuning example.

Section **III-B** presents our efficient approach to emotion classification through a Metric Projector. We detail how we delegate the task of emotion classification to an integrated metric-learned cross-modal projector, addressing challenges in fine-grained classification faced by traditional MM-LLMs and achieving more efficient training. This section explains the architecture and training process of our Metric Projector, emphasizing its role in enhancing the overall performance of our system.

Finally, in Section **III-C**, we describe TinyEmo, our complete system that integrates the dataset and classification approach. We discuss how we combine these elements to create a family of models with different LLM backbones, ranging in size from 0.70B to 3.21B parameters. This section outlines our training strategy, explaining how we leverage the TinyLLaVA framework to easily integrate various vision encoders and language model backbones, and details the two-stage training process that enables our models to perform emotional reasoning and classification.

#### A. Emotional Visual Instruct Dataset

Our dataset is designed for both pre-training and fine-tuning phases. The pre-training dataset incorporates three tasks: (1) Image Captioning – to learn the broad content of an image; (2) Visual Question Answering (VQA) – to learn important spatial

properties of images; such as color and objects, and (3) Sentiment Question Answering (SQA) – to handle our downstream tasks on visual sentiment analysis; providing the LLM with broad knowledge across multiple visual and emotional contexts.

To generate the corresponding questions and answers for the three pre-training tasks, we employed Bunny-v1.0-3B [60], a light-weight open-source multimodal LLM built upon SigLIP [61] and Phi-2 [49], [62], which at the moment of building the dataset was the model of its size with highest score on perception sub-tasks, as noted on the MME benchmark [63]. This process was applied to the entire WEBEmo [14] train dataset, comprising 213,952 images labeled according to Parrott's taxonomy [3]. As a result, our pre-training dataset consists of 641,856 single-turn, single-task conversation records (three tasks per image), with tasks presented in random order to avoid the model to overfit on the order in which the tasks are presented, thus mitigating potential implicit bias.

For fine-tuning our MM-LLM to generate Emotional Reasonings from images, we transform the pre-training dataset into an instruction-following format. Each record uses the LLaVA-Instruct-150K [8] dataset format “<image>\n{Instruction}”, with the sentiment answer from the pre-training dataset as the target response for the agent providing both the reasoning and predicted label in the same answer: “Reasoning: <sentiment answer>\n Predicted Label: <pred label>”. For an example format on how the instruction used in fine-tuning is built, refer to Appendix A-B.

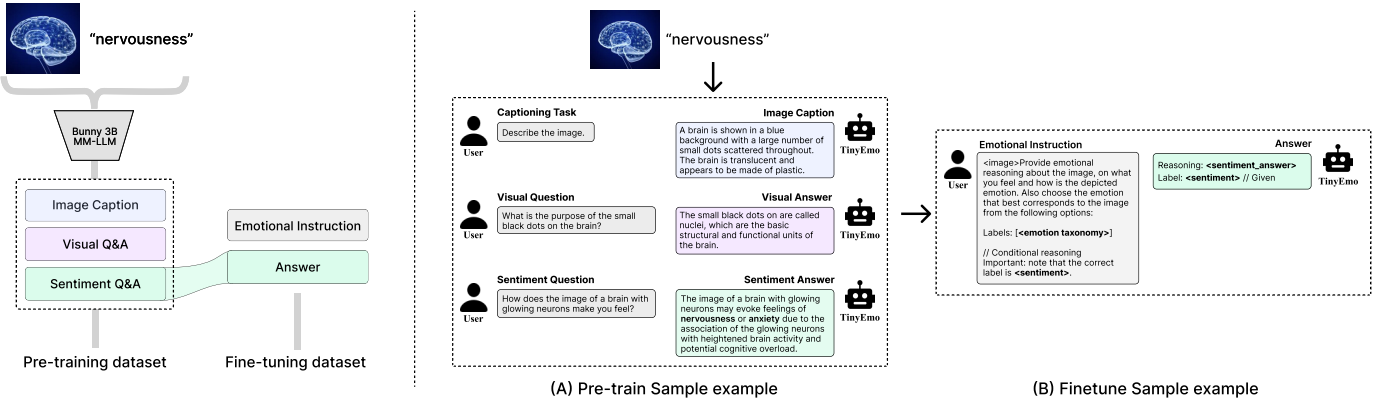


Fig. 1. Our dataset is composed of two datasets, the pre-training dataset is made to give our text-only LLMs foundational visual knowledge, and the fine-tuning dataset which is derived from the pre-training dataset by posing it as instruction-following format. (A) Using Bunny 3B [60] we generate three VQA tasks in Question-Answer format. During training, we present this questions in random order and the LLM has to learn how to appropriately answer them. (B) In the fine-tuning dataset, we do not generate any new samples, instead we use the already existing pre-training dataset's Sentiment Answer as the target response.

In addition to the synthetic data, we incorporated a small subset of 1,500 high-quality synthetic (HQs) emotional reasoning samples generated using Claude 3.5 Sonnet, a top-performing closed-source LLM as per Chatbot Arena [64], a crowd-sourced LLM evaluation platform. While our larger synthetic dataset prioritizes scale, this HQ subset offers us an opportunity to study the impact such data may have in our model. Our fine-tuning dataset consists of 215,452 single-task conversations, which includes one task per image from the original 213,952 WEBEmo images plus the 1,500 HQs samples.

In this fine-tuning stage, a prompt is shared across all samples, in contrast with the prompts of the pre-training dataset where each sample had its very own generated question different from the rest. This distinction between pre-training and fine-tuning prompts is illustrated in Appendix A. Hence, if we denote the image of a sample  $k$  as  $X_v^{(k)}$  with a common shared instruction as  $X_i \forall k$ . Our dataset consists of pairs with prompts  $X_p = \{X_v^{(k)}, X_i\}$  and answers  $X_a$ . If we define our model as  $f_\theta$ , where  $\theta \in \Theta$  contains its pre-training parameters, we want to minimize the loss between the generated response and the target answer.

$$\arg \min_{\theta \in \Theta} \mathcal{L}(f_\theta(X_p), X_a). \quad (1)$$

Note that the same formulation can be applied to the pre-training dataset, this time though, instead of instructions we now have questions  $X_q$  that vary for each sample  $k$ , thus in this case the set of prompts  $X_p$  can be defined as  $X_p = \{X_v^{(k)}, X_q^{(k)}\}$ .

### B. Emotion Classification: Metric Projector

As mentioned in the Related Work section (II), MM-LLMs struggle with fine-grained classification because they are trained on less data compared to the vision encoder (e.g. CLIP), resulting in the LLM being worse in fine-grained object classification tasks [13]. To address this flaw, we propose the delegation of the emotion classification task to an added metric-learned cross-modal projector, which will be trained solely on visual emotion classification. By maintaining two projectors, and detaching the classification and reasoning tasks, we expect the LLM to be better posed to learn complex reasoning on emotional content, now that it has only one task to focus on.

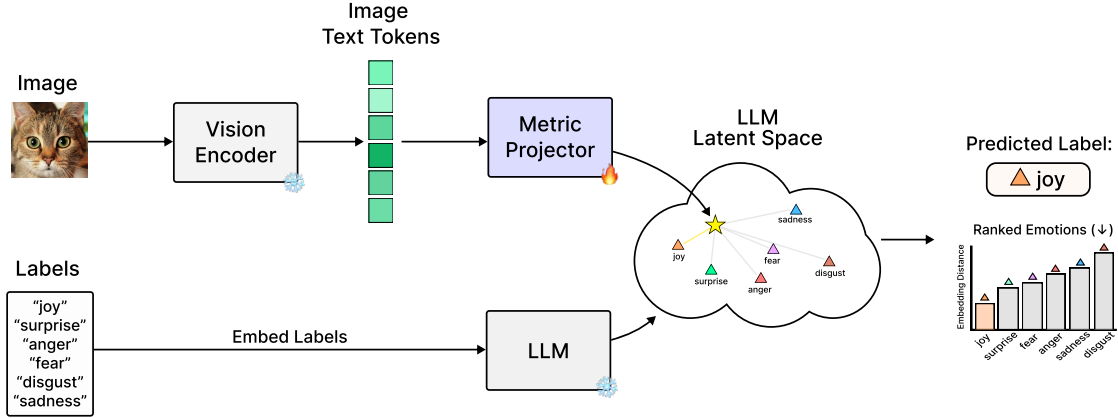


Fig. 2. Our proposed architecture to perform emotion classification. The image goes through the vision encoder (frozen) and gets projected to the target LLM embedding space with our Metric Projector. The labels associated with the image are directly embedded onto the same space with the LLM. Both embeddings are L2 normalized. We retrieve the closest label via cosine similarity. This approach also allows us to get a rank of emotions, by measuring distances, this can serve as a potential indicator of how each emotion of the taxonomy is represented in the given image.

Our implementation (Figure 2) consists of a 2-layer Multi-Layer Perceptron (MLP) with an initial layer that up-scales the vision encoder feature dimension to match the text embedding dimension, followed by a batch normalization layer and a GeLU [65] activation function, introduced to break linearity and capture more complex patterns. We then incorporate a drop-out layer to mitigate over-fitting in intermediate representations, and conclude with a final linear layer that maintains the input and output dimensions of the LLM embedding space. The output of this MLP is then L2 normalized to obtain the image projected embeddings.

Our approach is further motivated by several factors. Cross-modal alignment through MLPs has demonstrated success in multi-modal LLM architectures. We compare our approach with a vision encoder CLIP ViT-L/14 [32] and a state-of-the-art small multi-modal large language model PaLI-Gemma-3B [66] in Table I, which shows the trainable parameter count. This efficiency enables fast computation and rapid iteration, especially with pre-computed visual features, and allows us to easily swap LLM backbones, aligning with recent advancements in text embeddings models with top-performing models going towards higher embedding dimensions as seen on the MTEB [67] benchmark.

Approach to classification	Vision Encoder	Projector	LLM	Trainable Params
TinyEmo approach (Ours)	⌘	✓	⌘	3M
Vision Encoder approach [32]	✓	-	-	428M
Multi-modal LLM approach [66]	✓	✓	✓	2,920M

TABLE I. Comparison of architectural approaches and trainable parameters for Emotion Classification task. ⌘ indicates a frozen component, ✓ indicates an active (trainable) component, and - indicates the component is not present. Our TinyEmo approach uses a frozen CLIP ViT-L/14 for vision encoding and a frozen LLM (TinyLlama-1.1B), with only the Metric Projector (MLP) being trained. The Vision Encoder approach (CLIP) uses its vision encoder (ViT-L/14) and text encoder in the same embedding space. The Multi-modal LLM approach (PaLI-Gemma-3B) trains the entire model end-to-end, including the vision encoder, cross-attention projector, and language model, resulting in significantly more trainable parameters.

To train the metric-learning projector, we employ contrastive learning to handle primarily two sets of embeddings:

- Image Embeddings ( $P_v$ ) derived from encoding images  $X_v$  with the vision encoder  $F_v$  and the projector  $P_v = g_\phi(F_v)$ , where  $\phi$  are the trainable projector parameters.
- Text Embeddings ( $P_t$ ) obtained by embedding the textual sentiment labels  $X_t$  of the associated images through the LLM  $P_t = f_\theta(X_t)$ .

Due to the nature of higher dimensional embeddings, we require metric learning to learn distances between different samples, accomplishing the goal of minimizing the distances between corresponding image and text embeddings while maximizing the distance between non-corresponding pairs. We employ two different strategies for this task. Our first approach implements a fully-contrastive loss using the NTXent loss formulation [68]. For a batch size of  $N$ , this can be formulated as:

$$\mathcal{L}_{P_v, P_t} = -\log \frac{\exp(P_v \cdot P_t^+ / \tau)}{\sum_{i=0}^N \exp(P_v \cdot P_t^{(i)} / \tau)} . \quad (2)$$

Where the query is the projected image embeddings  $P_v$  and the keys are represented by the embedded textual labels  $P_t$ . The positive keys, defined as  $P_t^+$ , correspond to the embedding of the label assigned to the image.

In our second approach we employ a semi-contrastive learning strategy that focuses solely on pulling same-label samples together, without explicitly pushing different labels apart. This is achieved by considering only the positive case of the cosine embedding loss. It leaves that the loss can be formulated as a simple cosine similarity, and since the embeddings  $P_v$  and  $P_t$  are L2 normalized, the cosine similarity can be thought as computing the euclidean distance.

$$\mathcal{L}_{P_v, P_t} = 1 - \cos(P_v, P_t) \equiv \frac{1}{2} \|P_v - P_t\|_2^2. \quad (3)$$

This two-strategy approach is motivated by the observation that our emotion-related embeddings in LLMs share semantic similarities and may be inherently too close in the embedding space to effectively form clusters, as this is out of our control we aim to maintain a flexible approach preferable when working with different LLM backbones.

### C. Putting it all together: TinyEmo

Having presented the dataset construction in Section III-A and introduced our approach for Emotion Classification using the Metric Projector in Section III-B, we now present how these components come together in TinyEmo. We detail the complete architecture and training strategy we follow to achieve this, as well as hypotheses that guide our experimentation.

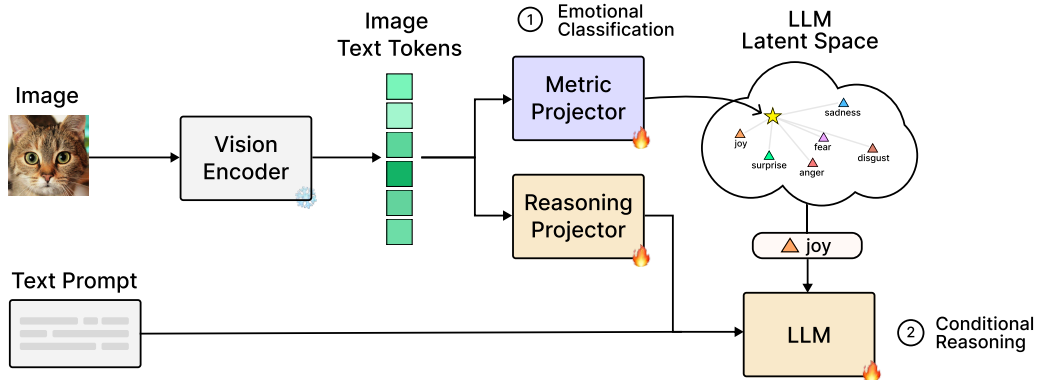


Fig. 3. TinyEmo is a multi-modal language model (MM-LLM) designed for both emotion classification and emotional reasoning. The flow of information is split into two steps: Emotional Classification and Conditional Reasoning. The image first goes through the vision encoder (frozen) and then gets projected to the LLM embedding space using our trained Metric Projector (Section III-B), where Emotional Classification is performed by retrieving the closest emotion label (Figure 2). Once the emotion label is predicted, it is appended onto the instruction (Section III-A) to guide the Conditional Reasoning stage, where the LLM generates the reasoning based on the predicted emotion label and the image itself.

TinyEmo leverages the TinyLLaVA [69], [70] framework to easily integrate various vision encoders and language models backbones. In Table II, we present the components we experimented with, focusing not only on the impact of parameters but also on validating two key hypotheses. First, we explore whether the trend of higher embedding dimensions improves performance, as seen in text-embedding models [67], holds true for emotion classification in multi-modal settings. Second, inspired by McKinzie *et al.* [31], we investigate the importance of image resolution in vision encoders.

Components	Model Names	Parameters ↓	Hidden dim.	Img. Res. / Seq. Len.	(Training Corpus, #)
Vision Encoders	DINOv2 ViT-L/14 (reg) [71]	304M	1024	224×224	(LVD, 142M Img)
	CLIP ViT-L/14 [32]	428M	768	224×224	(WIT, 400M I-T)
	CLIP ViT-L/14@336 [32]	428M	768	336×336	(WIT, 400M I-T)
	SigLIP-So400m/14 [61]	878M	1152	384×384	(WebLI, 10B I-T)
Language Models	OpenElm-270M-Instruct [72]	272M	1280	512	(Various <sup>1</sup> , 1.8T tok.)
	OpenElm-450M-Instruct [72]	457M	1536	512	(Various <sup>2</sup> , 1.8T tok.)
	TinyLlama-1.1B [73]	1.10B	2048	512	(Various <sup>2</sup> , 3.0T tok.)
	Phi-2 [66]	2.78B	2560	512	(Various <sup>3</sup> , 1.4T tok.)

TABLE II. Components used in TinyEmo. For Vision Encoders, training data is reported as Image-Text (I-T) pairs, except for DINOv2 which is trained on images only. For Language Models, we report the number of tokens processed during training, which may exceed the dataset size depending on epochs.

Inspired by LLaVA [38], our training strategy follows a two-stage approach, with an added requirement of training the classification pipeline beforehand:

<sup>1</sup>OpenELM models were trained on RefinedWeb [74], deduplicated PILE [75], a subset of RedPajama [76], and a subset of Dolma v1.6 [77].

<sup>2</sup>TinyLlama was trained on SlimPajama [78] and StarCoderData [79].

<sup>3</sup>Phi-2 was trained using a combination of NLP synthetic data created by GPT-3.5 and filtered web data from RefinedWeb and SlimPajama, which was assessed by GPT-4 [80].

### Stage 1. Emotional classification training

This pre-eliminary stage focuses on training our Metric Projector (Section III-B) on emotional image classification task. It is crucial for the visual-text alignment. Given the pooled representation of our image generated by the vision encoder,  $F_v$ . We project these tokens using our trainable metric projector  $g_\phi(F_v)$ , where  $\phi$  represents the trainable parameters of the projector. This projection results in an embedded representation of the image in the LLM latent space,  $P_v$ . We also obtain the latent representation of the textual labels, which will be defined by embedding the image's emotional taxonomy through the LLM, which we denote by  $P_t$ . We then apply contrastive learning with either of our approaches from Equations 2 and 3, and retrieve the predicted label using cosine similarity. Following a similar formulation as we did with Equation 1, we now have:

$$\arg \min_{\phi \in \Phi} \mathcal{L}(g_\phi(F_v), P_t), \quad (4)$$

Notice that, due to the conditional reasoning approach we have taken, this stage will greatly affect the rest of the system.

### Stage 2. Emotional reasoning training

Building upon the previous stage, we now focus on developing the reasoning capabilities of our model. In the first stage we concentrate on training the reasoning projector using our pre-training dataset, for foundational tasks for general vision capabilities such as Image Captioning, Visual Question-Answering (VQA), and more downstream tasks such as Sentiment Question-Answering (SQA).

The second stage, we follow LLaVA [38] guidelines and we simultaneously fully fine-tune both the reasoning projector and the LLM with our Emotional Visual Instruct tuning dataset. This results in the model generating emotional reasoning, with the distinction of our approach: Conditional Reasoning, where we first predict the sentiment label assigned to the image with the Metric Projector, and we insert that predicted label onto the prompt to generate our reasoning (this can be seen on Figure 1, where we append this information at the end of the Emotional Instruction prompt). This approach is what makes our method be more efficient and stable during training and inference, as the LLM has to only focus on the reasoning task because the classification part is already given. Hence, given a prompt that contains an image and an instruction  $X_p = \{X_v^{(k)}, X_i\}$ , the image  $X_v$  is encoded and projected by our metric projector, for which an emotion label is predicted  $g_\phi(F_v)$ ; thus the generation of the reasoning will be subject as a conditional with respect to this label:

$$\begin{aligned} f_\theta(X_p) \rightarrow f_\theta(X_p \mid g_\phi(F_v)), \\ \arg \min_{\theta \in \Theta} \mathcal{L}(f_\theta(X_p \mid g_\phi(F_v)), X_a). \end{aligned} \quad (5)$$

By off-loading the classification to a specialized part of our system and then generating the reasoning upon that, we allow the LLM to dedicate exclusively to the task of reasoning. Moreover, this approach aligns with recent findings [13] suggesting that MM-LLMs often struggle with fine-grained classification tasks.

## IV. EXPERIMENTS

### A. Ablation Study: Impact of Training Dataset Selection on Emotion Classification

Regarding our selection of datasets, we denote four main taxonomies present in emotion classification datasets. Datasets using Ekman's [2] six basic emotions (*anger, disgust, fear, joy, sadness, surprise*) are denoted with '6'. These include EmotionROI [23], Emotion6 [14], Abstract [18] and ArtPhoto [18]. Additionally, EmoSet [15] and FI [17] (Flicker-Instragram) datasets employ Mikels [81] eight emotion taxonomy (*amusement, anger, awe, contentment, disgust, excitement, fear, and sadness*), labeled as '8a'. UnbiasedEmo [14] dataset, designed for cross-domain evaluation for WEBEmo, uses a similar eight emotion taxonomy but replaces *disgust* with *love*, corresponding to the second hierarchical level of Parrot's. We named the latter with '8b'. Finally, WEBEmo [14] is annotated with Parrott's full three-level hierarchy [3] with 25 emotion categories and is denoted as '25' in our study.

Our approach to emotion classification through the implementation of a Metric Projector, featuring 3M trainable parameters, coupled with our dual approach of semi and fully contrastive learning (detailed in Section III-B), allow us to incorporate a wide variety of datasets while keeping computational requirements at minimum. This contrasts with approaches like EmoVIT [10], which relied on the MM-LLM and was limited to using less than 50% of the EmoSet dataset due to computational constraints (as noted in their limitations section). In terms of training methodology, we experimented with continual learning techniques such as Elastic Weight Consolidation to be able to train one dataset at a time and avoid catastrophic forgetting. However, we found joint learning to be the most effective approach. Our process involves projecting an input image features to the LLM embedding space, then embedding the labels and retrieving the closest matches via cosine similarity. Importantly, our prototypes (emotion labels) remain fixed, as we keep the LLM frozen, meaning the embeddings do not change during training.

We also explored implementing a complementary projector to allow dynamic grounding of textual labels, but we achieved better training results with the fixed approach. As training corpus we discarded evaluation datasets, such as UnbiasedEmo, and introduced one dataset of each taxonomy available.

Training datasets			Evaluation datasets								Metrics	
EmoROI 6	EmoSet 8a	WEBEmo 25	EmoROI 6	EmoSet 8a	WEBEmo 25	Emotion6 6	FI 8a	ArtPhoto 6	Abstract 6	Unbiased 8b	Total Accuracy	Zero-shot Accuracy
✓	✓	✓	76.77	31.77	10.78	87.04	23.83	36.23	15.04	53.04	41.81	43.04
			45.29	83.6	9.84	45.12	64.98	40.2	26.55	55.83	46.42	46.54
			38.55	27.18	42.23	39.9	26.46	23.7	15.49	56.62	33.77	32.43
✓	✓	✓	69.19	83.7	11.55	74.75	64.22	40.32	26.11	57.9	53.47	52.66
			72.73	30.18	42.12	78.11	23.12	28.66	13.27	56.39	43.07	39.91
			46.3	83.77	41.54	44.95	64.52	40.32	28.76	64.11	51.78	48.53
✓	✓	✓	70.54	83.82	41.41	77.27	63.1	40.2	36.73	64.11	<b>59.65</b>	<b>56.28</b>

Held-In data

Zero-shot

TABLE III. The performance TinyEmo-3.21B metric projector in emotion classification when we train our model on different combinations of datasets. We follow the same convention established by EmoVIT and denote as Held-In data the datasets we train on, for which we evaluate later on their corresponding test sets. To ensure fair comparison across different training configurations, we define two key metrics: Total Accuracy and Zero-shot Accuracy. Total Accuracy represents the mean of all test accuracies, including both Held-In and Zero-shot datasets. Zero-shot Accuracy focuses on generalization capabilities, calculated as the mean accuracy across Emotion6, FI, ArtPhoto, Abstract, and UnbiasedEmo datasets.

Table III shows valuable insights. Our joint training dataset comprising all three datasets consists of 309,819 samples in total. EmotionROI with just 1,346 samples accounts for the 0.45% of it, EmoSet with 94,481 samples accounts for the 30.50%, and finally WEBEmo with 213,952 accounts for a significant 69.05%.

Evaluating the individual impact of each dataset (see Appendix B for details), we can see EmoSet yields the best results with 46.42% and 43.04% of Total Accuracy and Zero-shot Accuracy, respectively. This is followed by EmotionROI which, surprisingly, despite its small size is able to generalize better than WEBEmo. We attribute this to the taxonomies on evaluation benchmarks, as none of them have the same taxonomy as WEBEmo, hence its impact is primarily shown on its own test set.

When considering complementary datasets, EmoSet stands out as the most effective one as when combined with either EmotionROI or WEBEmo is able to improve results with respect the individual baselines. The combination of EmotionROI and EmoSet achieves 53.47% and 52.66% of Total Accuracy and Zero-shot Accuracy. Thus, our model demonstrates a significant benefit from the introduction of Few-Shot data, as we can see by the complementary impact of EmotionROI, increasing accuracy by a +23.9% on its own test set, and +29.63% on Emotion6, and even has impact on unrelated taxonomies such as WEBEmo or UnbiasedEmo that increases by a +1.71% and +2.07%, respectively.

Similarly, EmoSet and WEBEmo combined together show improvements in performance. In contrast, the combination of EmotionROI and WEBEmo, without EmoSet, actually worsens results compared to EmotionROI alone. We attribute this decline in performance to the gap between 6 emotion taxonomy of EmotionROI and the 25 emotion taxonomy of WEBEmo. Finally, the best overall performance is obtained by the combined approach of the three datasets, achieving 59.65% Total Accuracy and 56.28% Zero-shot Accuracy. Our model benefits from the inclusion of more data, and can appropriately yield good results on other taxonomies. This showcases the importance of Few-Shot data and suggests that the quality and diversity of training data are more important than the quantity. Despite WEBEmo accounting for nearly 70% of data, its overall impact turned to be smaller than EmotionROI accounting for a mere 0.45%.

### B. Ablation Study: Impact of Model Components on Emotion Classification

The flexibility of TinyEmo not only allows us to incorporate multi-taxonomy data effectively, but also enables us to easily swap and evaluate different model components at will. We aim to explore the relationship between model parameters and the individual core components, how these models scale and their impact on zero-shot accuracy for the downstream task of emotion classification.

As detailed in the methodology section (Table II), we experiment with a diverse set of vision encoders and LLM backbones in our TinyEmo variants. For vision encoders, we are particularly interested in CLIP ViT-L/14@336 and SigLIP-So400m/14 due to its increased image resolution size (336×336 and 384×384, respectively) compared to the regular 224×224, and DINOv2, which is pretrained without supervision solely on images for computer vision tasks such as segmentation. We compare these against standard CLIP models. Regarding LLM backbones, we focus on small models like OpenELM (270M-450M) instruct versions, TinyLlama, which is trained on 3T tokens, and Microsoft Phi, considered the best LLM of its size at the time of our experiments. To evaluate the zero-shot accuracy of our TinyEmo variants, we follow the same evaluation protocol as in the previous section, training each variant on the optimal combination of datasets identified in the dataset selection study and reporting the average zero-shot accuracy across the zero-shot datasets (Emotion6, FI, ArtPhoto, Abstract, and UnbiasedEmo).

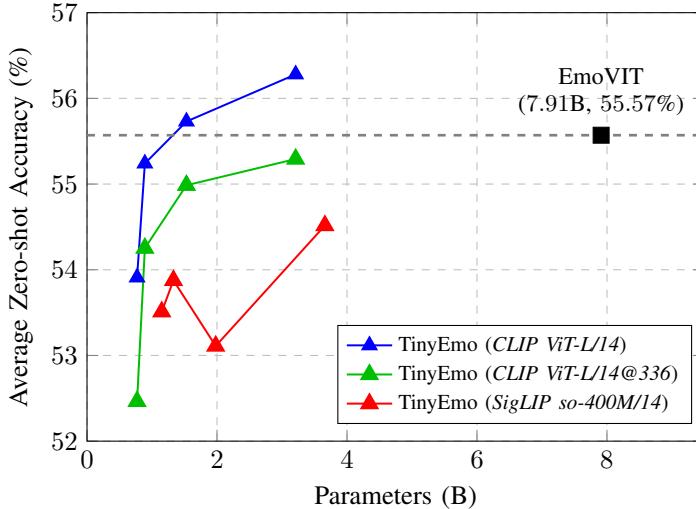


Fig. 4. Ablation study of parameters. Each line represents a specific vision encoder, with markers indicating the LLMs. The order of the LLMs is consistent: OpenELM 270M, OpenELM 450M, TinyLlama, and Phi-2. EmoVIT model is included as reference.

Vision Encoder	LLM	Params	Zero-shot
CLIP ViT-L/14	OpenELM-270M	0.77	53.91
	OpenELM-450M	0.89	55.24
	TinyLlama	1.53	55.73
	Phi-2	3.21	56.28
DINOv2 (reg)	OpenELM-270M	0.58	44.46
	OpenELM-450M	0.76	44.01
	TinyLlama	1.41	42.96
	Phi-2	3.08	45.25
CLIP ViT-L/14@336	OpenELM-270M	0.77	52.46
	OpenELM-450M	0.89	54.25
	TinyLlama	1.53	54.98
	Phi-2	3.21	55.29
SigLIP-So400M/14	OpenELM-270M	1.15	53.51
	OpenELM-450M	1.33	53.87
	TinyLlama	1.98	53.11
	Phi-2	3.66	54.51

TABLE IV. Average zero-shot accuracy and number of parameters for different combinations of vision encoders and LLMs.

Figure 4 serves as scaling analysis as for the CLIP visual encoders there is a consistent positive relationship between parameters and zero-shot accuracy. Suggesting that increasing the model size generally leads to improved performance in emotion classification.

Moreover, despite CLIP ViT-L/14 using a lower image resolution of  $224 \times 224$ , outperforms both the CLIP ViT-L/14@336 and SigLIP-So400M/14 encoders, which use higher resolutions of  $336 \times 336$  and  $384 \times 384$ , respectively. This challenges the hypothesis from Section II [33] on image resolution being a key factor. Also, the performance of CLIP ViT-L/14 compared to encoders with larger embedding dimensions, such as SigLIP-So400M/14, also disregards the hypothesis from Section III-B on the trend of text-embedding models increasing hidden embedding sizes. In Table IV, the DINOv2 (reg) encoder underperforms all other vision encoders across all LLM backbones. For clarity, we have not included the DINOv2 (reg) results in Figure 4.

### C. Ablation Study: Impact of Pseudo-label Augmentation on Emotion Classification

Based on Bustos *et al.* [35], who incorporates a 5-synonym augmentation for WEBEmo labels in their CLIP-E model, we explore a similar approach to enhance our model generalization towards capturing more complex emotional relationships outside the pre-established taxonomies. In our experimental setup, we augment the WEBEmo dataset by adding 3 synonyms to each of the 25 original emotion labels, resulting in a total of 100 labels. During training, we employ a random label replacement, with a 50% chance of replacing original labels with a random synonym. We provide the full list of synonyms used for augmentation in Appendix C.

Models	Architecture	Normal		+3x Synonyms	
		Held-In	Zero-shot	Held-In	Zero-shot
TinyEmo-700M	CLIP ViT-L/14 + MLP + OpenELM-270M	60.98	53.91	63.39 (+2.41)	57.87 (+3.96)
TinyEmo-880M	CLIP ViT-L/14 + MLP + OpenELM-450M	63.76	55.24	62.02 (-1.74)	54.74 (-0.50)
TinyEmo-1.53B	CLIP ViT-L/14 + MLP + TinyLlama-1.1B	64.87	55.73	64.85 (-0.02)	56.13 (+0.40)
TinyEmo-3.21B	CLIP ViT-L/14 + MLP + Phi-2	65.26	56.28	64.09 (-1.17)	56.99 (+0.71)

TABLE V. Comparison of TinyEmo models trained normally and with 3x synonyms. Results show Held-In and Zero-shot average accuracies (%) for normal training and with 3x synonyms. Parentheses show the difference, with green indicating improvement and red indicating decline.

Table V showcases the impact of the pseudo-label augmentation. As we might expect, there is a decline in held-in evaluation performance for most models, attributed to the increased complexity of training with additional labels. There is a significant improvement in zero-shot performance across most of the models, particularly pronounced for the smallest model, TinyEmo-700M, which shows substantial gains in both held-in (+2.41%) and zero-shot (+3.96%) scenarios.

These results completely debunk our hypothesis made in Section III-B, which suggested that larger embedding size would lead to better classification performance. As our model, TinyEmo-700M (with embedding size of 1024), achieves the best zero-shot performance when augmented with synonyms, outperforming the larger versions.

#### D. Qualitative analysis of Emotional Reasoning

Emotional reasoning remains an underexplored area with few datasets and lack of metrics to assess the emotions present in text generation. This is due to the challenge of having to evaluate emotional reasoning text, as it lacks a “correct” answer and multiple interpretations are equally valid.

We compare emotional reasoning capabilities of three LLaVA v1.5 7B variants: a baseline, a model fine-tuned on Affective Explanations, which contains emotional reactions and explanations for 85,007 images provided by 6,283 annotators, and a model fine-tuned with our Emotional Visual Instruct dataset. With this we want to qualitatively assess the difference between models trained on human-annotated data and those trained on synthetic data. All experimental runs were trained for 3 epochs using 45,000 image-text pairs for each dataset. Our LoRA configuration included learning rate of 2e-4 with cosine scheduler and 3% warmup, batch size of 32 with bf16 precision. During inference, we use the 4-bit quantized version of the merged LoRA weights.

Aff. Exp. Image (Held-out sample)	LLaVA v1.5 7B (Baseline)	LLaVA v1.5 7B (Affective Explanations)	LLaVA v1.5 7B (TinyEmo Instruct)
	<p>The image features a single red rose placed in a small glass vase on a wooden table. The rose is the main focus of the scene, and its vibrant color and delicate petals create a sense of <b>beauty</b> and <b>elegance</b>. The wooden table adds a warm and natural touch to the setting. The simplicity of the arrangement, with just one rose and a single vase, can evoke feelings of <b>tranquility</b> and <b>serenity</b>, making it an ideal setting for a quiet moment or a thoughtful gesture.</p>	<p>The red rose is <b>beautiful</b> and the vase is <b>elegant</b>.</p>	<p>The image of a red rose on a wooden table evokes feelings of <b>affection</b> and <b>love</b> because the rose is a symbol of <b>love</b> and the wooden table represents a sense of <b>warmth</b> and <b>comfort</b>.</p>

Fig. 5. Comparison of emotional reasoning for the image of a held-out sample of Affective Explanations by LLaVA v1.5 7B fine-tuned variants. All models were fine-tuned and subsequently inferred using the prompt: “<image>\nDescribe what you see in the image and how it makes you feel.”. We highlight in red emotions or affective terms related to the emotional meaning of the image.

The baseline LLaVA model provides a verbose response, focusing on image captioning with precise emotional elements. The Affective Explanations tuned model generates a short response, lacking depth in both visual foundational knowledge and downstream emotional analysis. Our TinyEmo Instruct model always starts by presenting a very subtle captioning followed by focused emotional reasoning that is able to link visual elements to specific feelings. It directly addresses the emotions evoked (*affection, love*) and provides reasoning for these feelings, linking the rose to *love* and the wooden surface to *warmth* and *comfort*.

The reason we opted to create our own dataset, rather than relying on Affective Explanations, was that we were not able to make it generalize effectively during the experimental runs. Even when training on the longest captions subset, our tuned experimental model struggled to generalize effectively. This led us to develop a synthetic dataset with a special focus on spatial analysis, visual questions, and emotional instruct-following data, in that order.

Furthermore, we observed that the LoRA fine-tuning resulted in a model that incorporates emotional nuances even in more general tasks such as image captioning. This overfitting to the downstream task of emotional reasoning demonstrates the model’s increased emotional awareness across various prompts. For a detailed comparison of emotional reasoning capabilities on generic tasks, see Appendix D.

The TinyEmo Instruct variant shows a tendency to personalize descriptions and interpret emotional content in images, even when not explicitly prompted to do so. This behavior contrasts with the Baseline variant, which tends to provide more rational, objective captions. While this emotional overfitting can be beneficial for tasks requiring emotional interpretation, it’s important to consider its impact on general-purpose image understanding tasks.

#### E. Quantitative Evaluation of Emotional Reasoning

Affective Explanations authors perform quantitative evaluation of their generated text using both traditional reference-based NLP metrics (BLEU, ROUGE-L, METEOR, SPICE) and reference-free metrics. On the latter they emphasize CLIPScore, which uses CLIP to measure text-image similarity by projecting both image and generated caption on CLIP hidden latent

space and measuring embedding similarity. Luckily, they also employ a middle-ground approach with Ref-CLIPScore that performs text-image similarity but takes into account the ground-truth annotated data, as a middle-ground between traditional NLP and reference-free metrics.

Metrics	Achlioptas <i>et al.</i> [26] Speaker Variants			LLaVA Fine-tuned on Different Datasets		
	Default	Emo-Grounded	Pragmatic	Baseline	Affective Explanations [26]	TinyEmo Instruct III-A
CLIPScore ( $\uparrow$ )	66.70	66.80	69.20	77.58	71.18	69.95
Ref-CLIPScore ( $\uparrow$ )	75.00	75.00	76.30	70.22	75.45	71.71

TABLE VI. Comparison of CLIPScore and Ref-CLIPScore metrics across different models. Left: Speaker variants from Achlioptas *et al.* [26]. Right: LLaVA v1.5 (7B) models, including the baseline and versions fine-tuned on 75k samples from different datasets: Affective Explanations [26] and our TinyEmo Emotional Instruct dataset (Sec III-A). LLaVA was fine-tuned using LoRA; 4-bit quantization was applied on inference. All LLaVA variants were fine-tuned and subsequently evaluated using the prompt “What does this image make you feel?”. Higher scores indicate better performance.

Table VI presents CLIPScore and Ref-CLIPScore results for the different variants, compared against Affective Explanations models. CLIPScore reflects image-text alignment, but it’s challenging to prove it specifically accounts for emotional content. The LLaVA v1.5 Baseline achieves the highest CLIPScore (77.58), likely due to its strong captioning abilities observed in the qualitative assessment. Interestingly, the Affective Explanations-tuned model, despite providing very short captions, outperforms our Emotional Visual Instruct dataset-tuned model, suggesting that brevity might be favored by these metrics.

For Ref-CLIPScore, which considers ground-truth annotations, the Affective Explanations fine-tuned model performs best (75.45), as expected from a model trained on the same dataset used for evaluation.

These results highlight the under-exploration of current metrics in evaluating emotional reasoning tasks. While they provide some valuable insights, they are hard to check whether they capture emotional impact or depth of the generated text.

#### F. Interpretability of textual embeddings

Our TinyEmo metric projector aligns two modalities in a single textual LLM embedding space, which have semantic meaning encoded into it, can we get to know more about what our projector has learned? Can we examine the concepts it associates with images? How can we use this embeddings to boost our performance?

To explore this questions, we selected any of the available zero-shot datasets on our evaluation suite, such as Emotion6, and an experimental projector run of TinyEmo-1.53B, which combines CLIP ViT-L/14 and TinyLlama. Upon closer examination of the accuracy for each emotion in the taxonomy (*surprise*, *sadness*, *disgust*, *fear*, *anger* and *joy*) we observed that the ‘*joy*’ class significantly under-performed compared to other emotions, with only 5.68% of accuracy. The TSNE visualization of the embedded images, with each of the emotions textual labels grounded, revealed that the problem was indeed with the textual representation, as ‘*joy*’ seems to be overlapping with ‘*surprise*’. Note that we do not take TSNE results for granted, we use them as possible approximations of potential problems we might be facing. In this case, it allowed us to try to explore alternative textual representations for the ‘*joy*’ concept.

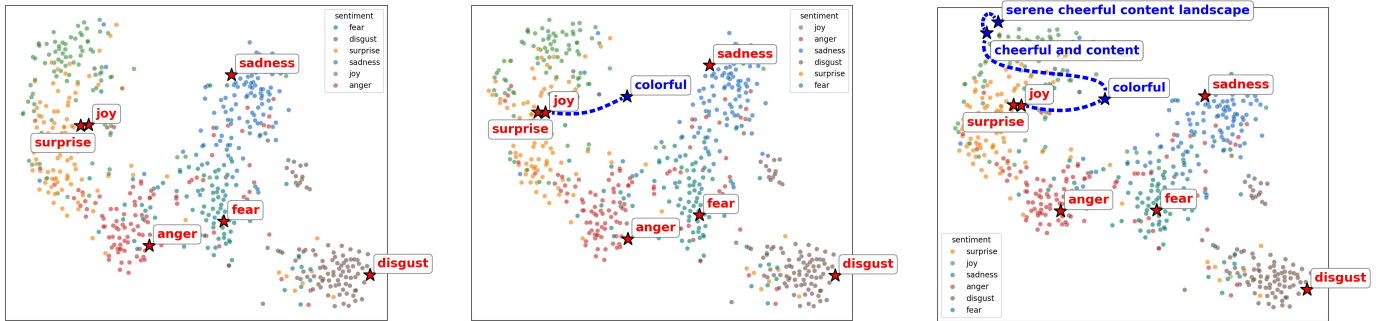


Fig. 6. TSNE visualization of the Emotion6 test dataset. Dots represent image embeddings, colored by their assigned emotion label, while stars indicate the textual embedding for each label. The figure highlights how replacing the label “*joy*” with alternative terms, such as “*colorful*”, shifts the embedding positions, showing that the model encodes semantic information in the embeddings.

Examining the *joy* images from the Emotion6 dataset, we noticed recurring themes such as flowers, birds, nature, sunsets, and landscapes, all characterized by having very colorful appearances. Replacing *joy* with “*colorful*” improved accuracy from 5.68% to 11.36%. Several tries revealed that replacing it with *cheerful* and *content* improved accuracy even more to 42.05%. This significant boost suggests that our model has learned to associate *joy* with concepts of cheerfulness and contentment, influenced by the WEBEmo dataset used in training which contains the latter labels. Interestingly, this changes caused a slight

Sentiments	Pseudo-label for “joy”			
	“joy” (Baseline)	“colorful”	“cheerful and content”	“serene cheerful content landscape”
Surprise	85.00	85.00	83.00 <span style="color:red">(-2.00)</span>	84.00 <span style="color:red">(-1.00)</span>
Sadness	83.17	83.17	83.17	83.17
Disgust	85.42	84.38 <span style="color:red">(-1.04)</span>	84.38 <span style="color:red">(-1.04)</span>	84.38 <span style="color:red">(-1.04)</span>
Fear	74.51	74.51	74.51	74.51
Anger	63.55	63.55	63.55	63.55
Joy	5.68	11.36 <span style="color:green">(+5.68)</span>	42.05 <span style="color:green">(+36.37)</span>	27.27 <span style="color:green">(+21.59)</span>

TABLE VII. Classification accuracies (%) with different pseudo-labels for “joy”.

decrease in ‘disgust’ accuracy (from 85% to 83%), despite the TSNE visualization showing these clusters far apart and not changing.

With this experiment, we have a way to empirically discover our projector learned textual representation for a given image, allowing us to ask, “What have you learned?” to the model. Moreover, we used this in our favour to boost accuracy performance. Finally, the fact that changes in the textual representations are reflected in the model retrieval proves that the embeddings maintain semantic meaning, towards a better understanding of the model internal representations.

#### G. Interpretability of visual embeddings

In the previous section we have seen how we can exploit the textual hidden representation on LLM embedding space to improve our labels prototypes and obtain better retrievals through grounding. There is semantic meaning encoded in the text representation. But how does this semantic encoding extend to visual inputs? Does our projection of ViT processed images into the LLM space preserve specific visual information? And how accurately does it align with related textual concepts?

We approached this questions by using a held-out sample image of UnbiasedEmo, obtaining its embedded representation resulted from passing it through a ViT encoder and Metric projector. We then compare this embedded representation in the hidden space to a diverse set of 200 textual prompts generated by GPT-4, which we categorize into three lists: related concepts, opposite concepts, and non-related concepts.

Embedded Image	Embedded Concepts	Top Concepts	Top Tokens																								
 UnbiasedEmo/anger_cat_5_2	<div style="display: flex; justify-content: space-around;"> <div style="text-align: center;"> <p><b>RELATED</b></p> <p>hiss scratch growl bite rage hostility ...</p> </div> <div style="text-align: center;"> <p><b>OPPOSITE</b></p> <p>purr contentment calm peaceful soft peace ...</p> </div> <div style="text-align: center;"> <p><b>NON-RELATED</b></p> <p>dog bird flower book computer forest ...</p> </div> </div>	<table> <tbody> <tr><td>1) feline anger</td><td>9) calmness</td><td>#1 anger</td></tr> <tr><td>2) angry cat</td><td>10) unhappy cat</td><td>#2 _anger</td></tr> <tr><td>3) rage</td><td>11) trusting</td><td>#3 _angry</td></tr> <tr><td>4) annoyance</td><td>12) fierce</td><td>#4 rage</td></tr> <tr><td>5) contentment</td><td>...</td><td>#5 ra</td></tr> <tr><td>6) violent cat</td><td>199) ballet</td><td>...</td></tr> <tr><td>7) irritation</td><td>201) sofa</td><td>#31999 _Buc</td></tr> <tr><td>8) feline frustration</td><td>202) cinema</td><td>#32000 Bas</td></tr> </tbody> </table>	1) feline anger	9) calmness	#1 anger	2) angry cat	10) unhappy cat	#2 _anger	3) rage	11) trusting	#3 _angry	4) annoyance	12) fierce	#4 rage	5) contentment	...	#5 ra	6) violent cat	199) ballet	...	7) irritation	201) sofa	#31999 _Buc	8) feline frustration	202) cinema	#32000 Bas	
1) feline anger	9) calmness	#1 anger																									
2) angry cat	10) unhappy cat	#2 _anger																									
3) rage	11) trusting	#3 _angry																									
4) annoyance	12) fierce	#4 rage																									
5) contentment	...	#5 ra																									
6) violent cat	199) ballet	...																									
7) irritation	201) sofa	#31999 _Buc																									
8) feline frustration	202) cinema	#32000 Bas																									

Fig. 7. Image embedding of an angry cat from UnbiasedEmo compared to 200 textual prompts which we split between related concepts, opposite concepts and non-related concepts. Top retrieved concepts like “feline anger”, “rage”, and “annoyance” confirm the preservation of visual information. Token retrieval results with “anger” being closest confirms that visual detail is retained in the embeddings.

In Figure 7 we show the top related concepts retrieved by our model, using cosine similarity. The majority of the top retrieved concepts are indeed related to the image content, with “feline anger”, “angry cat”, and “rage” topping the list. There are some visual specific concepts for which we have not trained on, like “annoyance” (4th retrieval), “irritation” (7th retrieval), and “fierce” (14th). This diverse emotional concepts and the fact that the model knows it is a “cat” shows that we have correctly inherited visual information encoded by the ViT. Opposite concepts like “contentment” also appear in the list which can be attributed to the training with emotional training we did, hence, potentially missing some visual information in favour to capture emotional content.

We went ahead and also embed the whole tokenizer vocabulary consisting of 32,000 unique tokens. The results align with the embedded concepts experiment, and we showcase how the retrieved tokens are indeed emotionally related with the sample image, with “anger” being the closest token (distance 0.33), followed by variants like “\_anger” (distance 0.50) or “\_angry” (distance 1.12), and related concepts such as “rage” (distance 1.15), “rages” (distance 1.19). During the tokenizer vocabulary embedding we are losing a lot of potential insights due to missing out on the combinations of tokens forming words, however we are not able to support such complexity of compute.

With this, we confirm that embeddings preserve some useful information about the image, inherited from the pre-trained vision encoder, despite not being trained to do so.

## V. RESULTS

### A. Emotion Classification

Building upon our findings from the ablation studies, we take advantage of our ease to introduce new datasets and employ the joint training detailed in Section IV-A, which have shown best performance in both Held-in and Zero-shot scenarios. We use a combined dataset of 309,819 samples, consisting of EmotionROI [23] (1,346 samples, 0.45%), EmoSet [15] (94,481 samples, 30.50%), and WEBEmo [14] (213,952 samples, 69.05%), each one with a different emotional taxonomy. For all TinyEmo configurations, we use the best-performing zero-shot vision encoder identified in Section IV-B: CLIP ViT-L/14 [32], with four different language models to create our TinyEmo variants: OpenELM-{270M, 450M} [72], TinyLlama [73], and Phi-2 [49]. Additionally, we incorporate the pseudo-label augmentation technique described in Section IV-C for the variants using OpenELM-270M and TinyLlama LLM backbones.

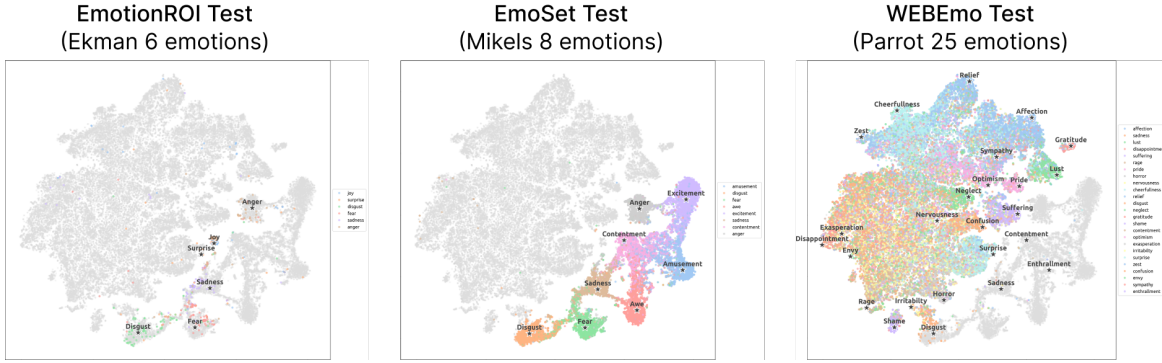


Fig. 8. TSNE visualizations of our held-in testing datasets (EmotionROI, EmoSet and WEBEmo). Each dataset follows a different taxonomy.

Figure 8 shows the TSNE visualization of our joint embeddings for the held-in testing of each dataset. In each visualization we highlight a different dataset, this allows us to evaluate how well these datasets adapt to each other taxonomies. EmotionROI, which is the one with the lowest representation (0.45%), adapts perfectly to the other corresponding bigger taxonomies and overlaps with EmoSet and WEBEmo. Supporting our observations made during Section IV-A that EmotionROI, when combined with other datasets, leads to significant improvements in accuracy. EmoSet, representing 30.50% of the data, has very well-defined clusters with clear relationships manifested in the form of paths or corridors from one emotion onto another, i.e. *anger* related with *excitement*. This reinforces the remark made on Section IV-A that EmoSet is a good complement to both EmotionROI and WEBEmo. Lastly, WEBEmo, despite constituting the majority of the training data (69.05%), presents a more complex embedding visualization. There is very subtle overlapping in *contentment* and *sadness* but the rest of emotions are spread. Some emotions have correctly developed a clusterized representation, such as *lust*, but a vast amount of images are organized in a central undifferentiable mass. This, again, aligns with our findings IV-A that WEBEmo, when used alone or as a complementary dataset, does not show big improvements.

Models	Params	EmotionROI 6	EmoSet 8	WEBEmo 25	Emotion6 6	FI 8	ArtPhoto 8	Abstract <sup>†</sup> 8	UnbiasedEmo 6
CLIP ViT-B/32 [32]	0.15B	42.17	—	11.25	46.53	49.97	—	—	—
CLIP-E Cross-Entropy [35]	0.16B	—	—	40.65	58.39	—	—	—	—
CLIP-E Contrastive [35]	0.16B	43.18	—	34.68	51.71	38.07	—	—	—
Flamingo [82]	—	21.72	29.59	9.21	21.67	14.91	17.50	3.57	—
LLaVA [8]	—	46.46	44.03	12.55	49.44	56.04	36.25	19.54	—
BLIP-2 [40]	—	50.51	46.79	20.10	50.00	57.72	36.25	28.57	—
Instruct-BLIP [7]	—	46.13	42.20	12.80	46.11	37.97	26.25	21.42	—
S <sup>2</sup> -VER [83]	—	—	—	—	54.00	51.80	—	—	78.70
EmoVIT [10]	7.91B	53.87	83.36	21.12	57.81	<b>68.09</b>	<b>44.90</b>	32.34	74.72
TinyEmo-700M* (3 Syn.)	0.70B	<b>71.72</b>	82.67	35.77	73.4	64.16	39.83	28.32	<b>82.40</b>
TinyEmo-880M	0.88B	67.68	83.45	40.14	70.37	60.47	41.19	27.88	76.29
TinyEmo-1.53B (3 Syn.)	1.53B	71.04	<b>83.92</b>	39.65	76.09	63.19	40.94	27.43	71.00
TinyEmo-3.21B	3.21B	70.54	83.82	<b>41.41</b>	<b>77.27</b>	63.10	40.20	<b>36.73</b>	64.11

TABLE VIII. Comparison of 4 different metric projector models for emotion classification. Our models were jointly trained on EmoROI, WEBEmo, and EmoSet to cover main taxonomies (6, 8, and 25 emotions), then benchmarked on other datasets in a zero-shot manner. All models were trained for 5 epochs with a batch size of 32, cosine learning rate scheduler and cosine embedding loss formulation (Eq 2) unless stated otherwise.

\* Trained using our fully-contrastive NTXent loss formulation (Eq 2).

† For the Abstract dataset, the label grounding was done with the following grounding text: “a scene evoking {emotion} to viewers”.

In Table VIII we provide a comprehensive comparison of TinyEmo metric projector for Emotion Classification with respect other approaches. We highlight with gray cell background those datasets on which each method has been trained, if any. We

include distinct approaches to compare with, including vision encoders (CLIP ViT-B/32), general purpose multi-modal large language models (Flamingo, LLaVA, BLIP-2, Instruct-BLIP). We also include emotion-specific methods that were trained with emotions in mind, we split these into tight integrations with CLIP, such as CLIP-E, which add fully-connected layers on top of the vision encoder and train with contrastive loss methodology, semi-supervised approaches (S<sup>2</sup>-VER), and specialized multi-modal LLMs for emotion recognition (EmoVIT).

Evaluating the zero-shot performance (Emotion6, FI, ArtPhoto, Abstract and UnbiasedEmo) the most capable model is TinyEmo-700M (57.62%) when augmented with pseudo-labels. Followed by our largest model TinyEmo-3.21B (56.28%). Both outperform the current state-of-the-art EmoVIT (55.57%) due to our ability to incorporate more data, enabled by our less computationally restrictive approach. This is particularly impressive given that our best-performing model has only 700M parameters compared to EmoVIT 7.91B total parameters. This shows a clear trade-off between model size and data to incorporate, where our models are smaller but leverage more diverse datasets to account for that.

Despite this, there are specific datasets where EmoVIT shows impressive results, especially considering the limited amount of data it was trained in. On FI and Abstract datasets, EmoVIT outperforms all other approaches, while we achieve the second best performance on them. For the Abstract dataset, we initially underperformed but discovered that embedding the text grounding labels with “a scene evoking {emotion} to viewers” drastically improved the results (see Section IV-F for more detail onto the textual interpretation of embeddings through different possible label groundings).

### B. Emotional Reasoning

In our approach for emotional reasoning, we allocate a significant amount of our model’s parameters to generate detailed textual explanations for emotional contexts. Taking TinyEmo-1.53B as an example, which combines CLIP ViT-L/14, two independent projectors for classification and reasoning, and TinyLlama as LLM, we actively train the reasoning projector and the LLM solely for reasoning. This results in 1.1B trainable parameters dedicated to reasoning (1.53B minus the 428M of the frozen ViT encoder). This stands in contrast with the emotional classification task, in which we allocate only the metric projector (3M training parameters) during training. It is remarkable that neither of our LLM backbones offered in our TinyEmo variants (OpenELM, TinyLlama and Phi-2) have any inherent vision capabilities; they are purely text-only LLMs. Despite training these models from scratch to acquire visual foundational knowledge, it is impressive how our TinyEmo models are able to capture visual details.

In Section III we discuss how we detach the classification task from the LLM to a Metric Projector, this allows for a more flexible approach that can incorporate more data and less computational requirement. In Figure 9 we show two types of reasonings; the “normal” reasoning, where the LLM is trained for classification and reasoning simultaneously, without employing the Metric Projector; and the “conditional” reasoning, where our Metric Projector first performs the classification, and then that label is given to the LLM to perform the visual emotional reasoning (hence the name of ‘conditional’ reasoning). In the latter task, the LLM is not trained for classification and can focus exclusively on reasoning.

Emotion6 Image	Normal Reasoning	Conditional Reasoning
	<p><b>Reasoning:</b> The image of the woman sitting alone on the sidewalk, <b>with her laptop open and her head resting on her hand</b>, evokes a sense of sadness because it portrays a solitary figure who appears to be lost or disconnected from the world around her. <b>The open laptop and the closed hand</b> suggest a sense of isolation and detachment, while the open hand indicates a sense of vulnerability or fragility.</p> <p><b>Predicted Label:</b> sadness</p>	<p><b>Reasoning:</b> The image of the homeless man sitting alone on the sidewalk evokes feelings of sadness and empathy because it portrays a vulnerable and helpless individual who is struggling to survive in a harsh and unforgiving world. The image highlights the harsh reality of homelessness and the struggles that people face in their daily lives.</p> <p><b>Predicted Label:</b> sadness</p>

Fig. 9. Comparison of emotional reasoning results using “normal” and “conditional” approaches. In the “normal” reasoning scenario, the TinyEmo model is trained to perform both emotion classification and emotional reasoning simultaneously, which can lead to inefficient training resulting in precision errors, as seen in the first sub-figure where the model incorrectly describes details not present in the image. In the “conditional” reasoning approach, the TinyEmo model is trained only for emotional reasoning task, where the classification is performed in advance by the Metric Projector. This method shows improvement with respect its predecessor as it correctly identifies the emotions and provides more precise reasoning.

As seen in Figure 9, this “conditional reasoning” approach allows for better and more accurate reasoning. In the “normal” reasoning, the caption is inaccurate, hallucinating details such as “her laptop open and her hand resting on her head” which

are evidently not present in the image. The conditional reasoning provides a more accurate caption for the visual content. Qualitatively, detaching classification and reasoning tasks constitutes an effective strategy for achieving better results at a lower computational cost.

EmoSet Image (Held-out sample)	EmoVIT [10] 7.91B params.	TinyEmo 1.53B params.	TinyEmo + HQ data 1.53B params.
	<p><b>Predicted emotion:</b> sadness</p> <p><b>Reason:</b> The image is a black and white photograph of an old, abandoned house in the middle of a field. The scene is desolate and eerie, which suggests a sense of sadness or melancholy.</p>	<p><b>Reasoning:</b> The abandoned, dilapidated house in the middle of a field evokes feelings of sadness and loss because it represents a once-thriving home that has been left to decay and fall into disrepair. The overgrown weeds and the dilapidated structure create a sense of abandonment and neglect, which can be emotionally distressing for viewers.</p> <p><b>Predicted Label:</b> sadness</p>	<p><b>Reasoning:</b> The abandoned, dilapidated house in the middle of a desolate, overgrown field evokes feelings of sadness and loss because it represents a place that was once vibrant and full of life, but now lies forgotten and neglected. The overgrown field and dilapidated state of the house symbolize the decay and abandonment of a once-thriving community, leaving behind a sense of loss and sadness.</p> <p><b>Predicted Label:</b> sadness</p>

Fig. 10. Comparison of emotional reasoning results between EmoVIT (7.91B parameters), our TinyEmo variant (1.53B parameters) using TinyLlama LLM, and TinyEmo with high-quality reasoning data (HQ data). The figure shows how each model interprets the image of an abandoned house. Notice the order in which we learned the classification and reasoning tasks. EmoVIT [10] first provides the predicted emotion and then its reasoning. In contrast, in our normal training scenario where the LLM is responsible for both tasks, the predicted label is indeed influenced by the given reasoning through chain-of-thought [84].

Figure 10 presents a comparative analysis of emotional reasoning capabilities across EmoVIT (7.91B parameters), our TinyEmo variant using TinyLlama (1.53B parameters), and an additional version of TinyEmo incorporating high-quality reasoning (HQ data) from Claude 3.5 Sonnet. By including both our standard dataset and a small subset of high-quality samples, we aim to evaluate the synthetic data at different qualities and the impact of it.

EmoVIT and both our Metric Projectors of our TinyEmo models, correctly classify the image as evoking “sadness”. EmoVIT’s reasoning provides a concise description, yet is able to capture the main visual elements (abandoned house, field) and is the only one to highlight the black and white colors on the image. The emotional interpretation is brief but accurate, linking the scene “desolate and eerie” with emotions “sadness or melancholy”. TinyEmo’s reasoning capabilities is more verbose and goes beyond basic description to interpret the emotional impact of the image. The phrase “once-thriving home that has been left to decay” introduces a temporal element, which is used to understand more nuanced emotions to a potential viewer such as “despair”. The mention of “overgrown weeds” shows good attention to visual detail that contribute to the emotional reasoning. TinyEmo has effectively positioned itself from the viewer’s perspective, capturing the evoked emotion, an aspect that EmoVIT lacks. TinyEmo variant with HQ data provides the most verbose caption of them all. It inherited a more sophisticated vocabulary from Claude, using more evocative language, i.e. replacing “vibrant and full of life” with “once-thriving”. However, it does not add significant new details compared to the TinyEmo reasoning without HQ data. Moreover, we observe that at its core, the HQ data version is repeating the same idea in both paragraphs: the home being abandoned contrasting it with the past. While the language is more elaborated, the underlying idea remains unchanged, hence no significant difference added despite more verbosity. Suggesting that the true value of adding HQ data may add more superficial improvements than substantial emotional analysis depth.

### C. Application: Metric projector as a semi-automated framework to detect bias

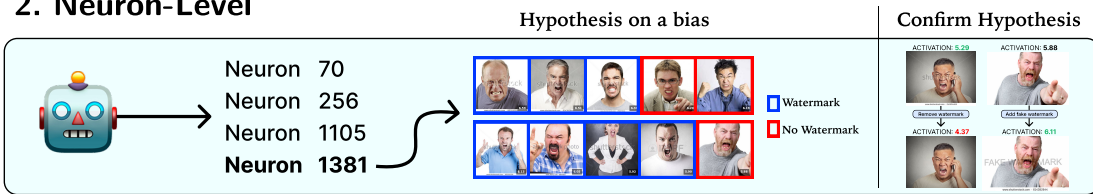
Our metric projector serves as a bridge between the vision transformer (ViT) and the language model (LLM), aligning the two modalities by mapping images to the textual embedding space. All images are required to pass through the projector, thus it is very conveniently positioned between two massive models that carry all cognitive task. The huge difference in size of the projector (3M training parameters) with respect ViT (CLIP ViT-L/14 has 428M parameters) and the LLM (the smallest LLM we are using has 700M parameters) provides a very unique opportunity, and to the best of our knowledge; not explored yet, that allows for indirect bias mitigation and interpretability of large complex systems from just the projector itself. One could think about the projector as the concept of “interpretability layer” offering indirect control that influence larger models.

To leverage this convenient positioning of the metric projector, we propose a semi-automated framework for detecting biases without any additional training needed. We maintain the emotion classification objective, but the use of metric learning on embeddings provides the flexibility to comply with the different steps of the procedure. Our approach is divided into three main steps. First, given an image we retrieve semantically and emotionally similar images. This step helps us narrow the sample space for further interpretability, make it more manageable. Next, using the subset of similar images, we examine individual neuron activations within our projector; “what neurons activate the most for the chosen samples?”. This granular approach

## 1. Image retrieval



## 2. Neuron-Level



## 3. Robustness

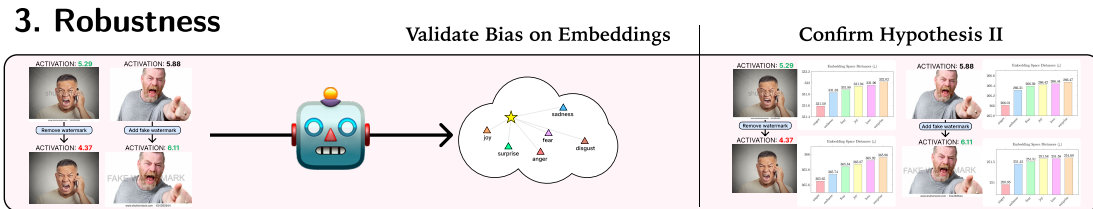


Fig. 11. A semi-automated framework for bias detection and interpretability in large models using the Metric Projector. Our proposed framework uses the metric projector as a bridge between the Vision Transformer (ViT) and the Language Model (LLM) to efficiently handle bias detection and interpretability experiments. Capable of performing (1) image retrieval, (2) individual neuron-level analysis, and (3) robustness validation.

help us, again, narrow the search for potential biases in the system and form our initial hypothesis. Finally, we extrapolate our individual neuron hypothesis to the entire model classification pipeline, to confirm whether the bias is being accountable for the ultimate classification decision, following a bottom-up approach. Each step progressively narrows the search space, to effectively detect and study biases that otherwise could end up obscured in the complexity of larger models.

1) *Image Retrieval*: Image retrieval is done by embedding all the set of sample images we wish to work with, in our case we embed the whole UnbiasedEmo dataset, and for a particular query image we select, we can retrieve the most similar images based on their embedding distances. Naturally, because of our training objective, the retrieved images have some shared emotional meaning, but despite this, there are some useful visual correspondences.

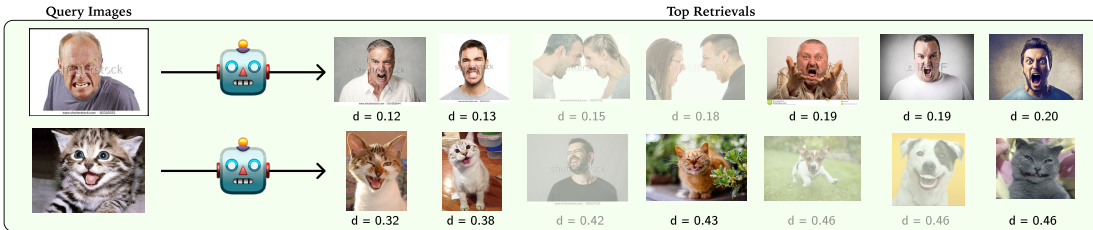


Fig. 12. Image retrieval results. Given a query image, we embed it and retrieve the most similar images by computing cosine distance, as embeddings are L2 normalized. We show two different retrievals for different query images, with the distance displayed below each retrieved image. This process helps narrow our sample size, allowing us to manually select retrievals of interest for potential bias investigation.

Important to note that this step is done by convenience to reduce our sample space of images, it is optional and requires human intervention. The goal is to reduce our sample size to a manageable subset relevant to our bias investigation. For instance, we might use this approach to explore potential biases in anger-related portraits (first row in Figure 12), or to examine the model behaviour with cats (second row in Figure 12).

2) *Neuron-level*: In this step, we take the chosen subset of images from the image retrieval phase and log the activations of all neurons in our metric projector. Our goal is to identify those neurons which activate the most in response to the images of interest. Once we have identified these high activation neurons, we can narrow our efforts to them and analyze the individual neuron behaviour across the whole dataset. All of this in favour of efficiency and computational requirements.

By iterating through this process, we can uncover neurons with specific roles. For instance, we discovered Neuron 1793 in Layer 0, which demonstrated peak activations for images related to Christmas (Figure 13). The top four activations are all

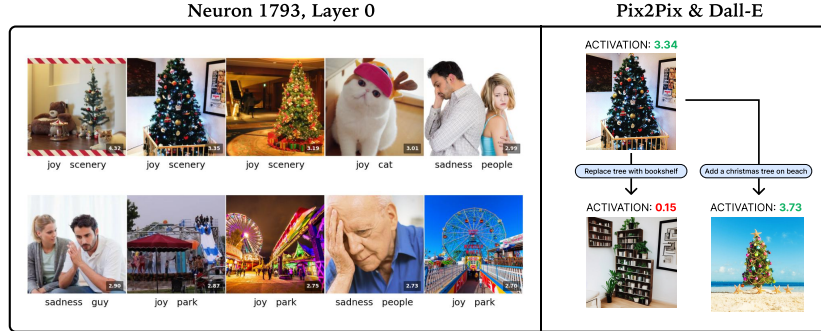


Fig. 13. “The Christmas neuron”. Left: Neuron 1793 specialized knowledge, inherited from the ViT projection. Its three highest activations correspond to the only subset of Christmas trees present in the UnbiasedEmo dataset. Furthermore, it strongly activates for a sample of a cat with a “rudolph hat”, suggesting that the neuron is able to recognize not just specific Christmas objects, but also associated holiday accessories. Right: Counterfactual experiment showcasing how when we replace the Christmas tree for a bookshelf the neuron activation drops from 3.34 to 0.15. Additionally, using Dall-E we generate an image of a Christmas tree on a beach which triggers the activation, reinforcing the idea that the surroundings is not what the neuron is looking at.

related with the festivity, and include the three only images of christmas trees in UnbiasedEmo dataset. Moreover, the fourth activation of a cat with a christmas-themed “rudolph hat” is particularly impressive, given that our model was trained from scratch for foundational vision tasks. This suggests that the neuron attention to specific visual details may be inherited from the vision encoder, CLIP; indicating that the alignment between the encoder and the metric projector is indeed having effect. This discovery allows us to create an initial hypothesis for a given neuron, in this case we can hypothesize that Neuron 1793 is specifically tuned to recognize “Christmas-related elements”.

To validate this individual neuron hypothesis, we use counterfactuals [59], [85] which involves editing images using tools like Pix2Pix [86], generative models like Dall-E [87], or even manual editing, to either support or reject our hypothesis by making visual changes. We then track the activation of the selected neuron of study in response to these newly edited images. For instance, using Pix2Pix we replace the Christmas tree, for the second most activated image, with a bookshelf. Despite the resulting edited image being similar in color and shape, it drastically reduced the neuron activation, falling off 3.34 to 0.15, hence, supporting our hypothesis. To further test if the neuron was responding to these images by the given surrounding context, we used Dall-E to create a Christmas tree on an unusual place such as a beach. This image caused an even stronger activation than the original, further reinforcing the idea that Neuron 1793 is specialized in recognizing Christmas trees, regardless of the surrounding environment.



Fig. 14. Neuron 1381 (Layer 0) activation analysis and counterfactual experiments. Left: Top 10 activating images from UnbiasedEmo dataset, predominantly showing angry individuals, with some of them containing clearly visible watermarks. Right: Counterfactual experiment using Pix2Pix and manual editing for which adding (or removing) a watermark, increases (or decreases) neuron activation.

Through repeated analysis, we identified interesting neurons that could result in potential biases. For instance, Neuron 1381 in Layer 0 have shown peak activations in response to images of angry individuals, a lot of them containing clear and visual watermarks. Hence, we formulate the initial hypothesis; “Does the presence of watermarks increase Neuron’s 1381 activation when detecting *anger*?” In the counterfactuals, we observe the activation drop from 5.88 to 4.37 when removing the watermark. Contrarily, when we add a fake watermark, we see how the neuron activates more than the original without a watermark. Thus, we confirm that, at neuron-level, images of angry individuals are sensible to the presence of a watermark in it.

3) *Robustness*: We now have detected a neuron-level bias, but is this bias present in the final classification decision made by our model? This robustness assessment examines both how the bias affects the embedding space and whether it significantly influences the ultimate emotion classification. If the edited image (e.g. the addition or removal of a watermark) makes the image closer to or further from the *anger* label in embedding space, we can say the bias is present. However, it only affects

decision-making if the classification of labels changes, which we can observe as the emotion distribution.

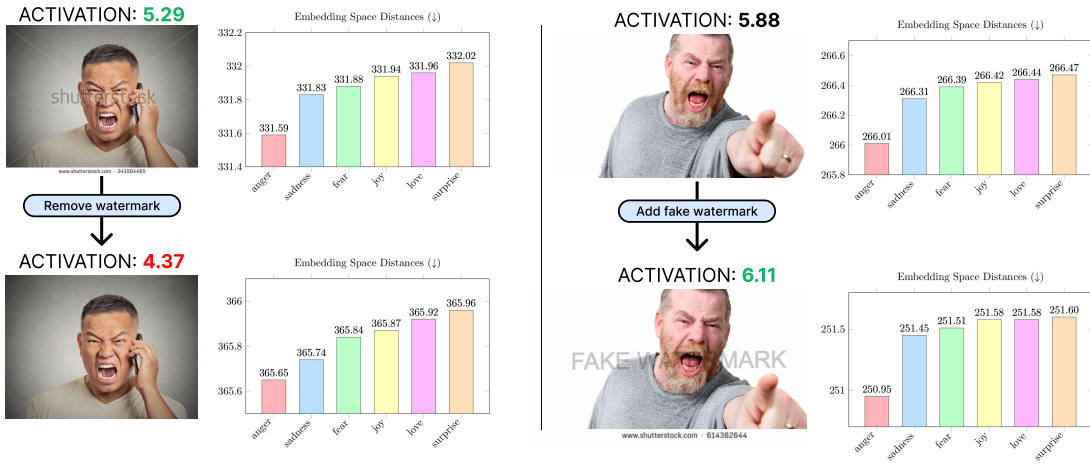


Fig. 15. Neuron activation and embedding space distances between image hidden representation and sentiment labels for samples from UnbiasedEmo dataset. Left: An angry man with a visible watermark (original) and with the watermark removed (counterfactual), labeled as *anger*. Right: Man shouting (original) and with a fake watermark added (counterfactual), labeled as *anger*. Bar charts show embedding distances to emotion labels, ranked in ascending order. The image is classified based on the label with the shortest distance. Note the changes in neuron activation and differences in embedding distances after watermark manipulation, indicating correlation between clearly visible watermark and the anger emotion.

As shown in Figure 15, in both cases, the addition or removal of the watermark alters the distance of the resulting embedded image representation to the “anger” label. This indicates that the bias does have some effect on the embedding space. However, to determine if this bias is influencing our final decision-making, we need to examine the emotion distribution. By plotting the distribution and corresponding embedding distances, we observe that overall, the distribution of emotions remains largely unchanged. This suggests that while the bias has a small effect on the embedding space, it is not significantly affecting our decision-making process. Having said this, we must remark that the model is not robust by definition; true robustness would imply that the counterfactual would have the same distance to the ‘anger’ label as the original image. However, because we are modifying the visual content of the image, this seems an unrealistic goal. Overall, we can confirm that the detected bias does not, ultimately, alter the final emotion classification.

## VI. CONCLUSIONS

In this paper we present TinyEmo, a family of small multi-modal language models designed for emotional reasoning and classification. We introduce three main contributions: (1) A synthetic Emotional Visual Instruct dataset for pre-training and fine-tuning, (2) A cross-modal Metric Projector for efficient emotion classification, (3) a multi-modal large language model (MM-LLM) for emotional reasoning, and (4) A semi-automated framework for bias detection in large multi-modal models.

The pre-training dataset effectively laid the foundational vision knowledge for our text-only LLM backbones, while the fine-tuning dataset has proven to generalize better than manually annotated alternatives for emotional reasoning (Section IV-D). We found that manually annotated datasets often fall short in generalization, mostly due to very short reasonings. While these reactions were often valid, they lacked the depth of emotional content required for our purposes. By creating our own synthetic dataset (Section III-A), we had more control over the process, leading to more efficient training and better generalization.

The Metric Projector, exclusively dedicated to the emotion classification task, reduced the training parameters, separated reasoning and classification objectives, and allowed for the inclusion of more training data with minimum computational overhead. We showcase our model’s few-shot capabilities, which makes the inclusion of new data easy, and regardless of the size of the included data it still has significant improvements on performance. For instance, EmotionROI, despite comprising only 0.45% of our training data, led to a performance increase of +7.87% in Total Accuracy and +7.75% in Zero-shot Accuracy when combined with other datasets (Section IV-A & Appendix B). Our Pseudo-label augmentation proved to be an effective strategy for better zero-shot performance on other taxonomies (Section IV-C). Our findings revealed that neither embedding size nor image size were as crucial as the quantity and diversity of training data.

Our Conditional Reasoning approach, where classification is performed by the Metric Projector before reasoning, led to more accurate and precise emotional interpretations, effectively reducing hallucinations and miss-classifications observed in the normal reasoning approach (Section V-B, Figure 9). This method, combined with our focus on foundational visual understanding tasks in the pre-training dataset, allowed our TinyEmo models to generate detailed emotional reasoning, despite being trained from scratch on visual knowledge. However, experiments with high-quality (HQ) data from Claude 3.5 Sonnet were inconclusive,

as the small sample size resulted in more verbose reasoning without improvements in emotional analysis (Section [V-B](#), Figure [10](#)).

Our semi-automated framework for bias detection (Section [V-C](#)) leverages the convenient positioning of the projector between the vision encoder and the language model. With fewer parameters than the models it aligns, the projector can be seen as an “interpretability layer”. We use a bottom-up approach, constantly narrowing our sample space through image retrieval, then forming an initial hypothesis of the presence of a bias at neuron level and finally extrapolating onto the end classification decision. Offering a new approach to understand and address biases in multi-modal AI systems, providing indirect control and influence over larger models.

Our findings revealed that data quantity and diversity were more crucial than embedding or image size for model performance. Overall, TinyEmo demonstrates the potential of efficient, targeted approaches for specialized architectures on downstream tasks.

## APPENDIX A

### PROMPTS

#### A. Pre-training Dataset Generation Prompts

The following prompts were used with Bunny-v1.0-3B [60] to generate the Questions and Answers for our TinyEmo Pre-train VQA Dataset.

##### Image Captioning Prompt

<image>Describe the image in 2-3 concise sentences. Include only the most critical visual elements to form a precise caption.

##### Visual Question Prompt

<image>Ask a question about the image that requires specific observation and analytical thinking to answer. Focus on a clearly visible aspect of the image.

##### Visual Answer Prompt

Provide a precise, to-the-point answer to the previously asked question about the image. Ensure your response directly references visual details.

##### Sentiment Question Prompt

<image>Generate a complex sentiment or emotional question about the image that prompts deep emotional reasoning from the respondent.

The associated sentiment label of the image: <sentiment>.

The question should be directly addressed to the individual answering, encouraging them to engage personally with the sentiment expressed in the image.

##### Sentiment Answer Prompt

Answer the above sentiment-based question based on the visual content and emotional reasoning. The associated sentiment label of the image: <sentiment>.

Avoid repeating the phrasing of the question; instead, focus on inferring and articulating the mood presented by the visual elements.

Summarize your answer in 2 concise sentences.

#### B. Emotional Fine-tuning Instruction Prompts

These prompts were used during the emotional fine-tuning phase of TinyEmo, implementing instruction tuning.

##### User

<image>Provide emotional reasoning about the image, on what you feel and how is the depicted emotion. Also choose the emotion that best corresponds to the image from the following options:

Labels: [<emotion taxonomy>]

// Conditional reasoning

Important: note that the correct label is <sentiment>.

##### TinyEmo

Reasoning: <sentiment\_answer>

Label: <sentiment> // Given

**APPENDIX B**  
**IMPACT OF EACH DATASET IN JOINT TRAINING CONFIGURATION**

We quantify the impact of each dataset by evaluating both Total Accuracy and Zero-shot Accuracy metrics as the difference between the joint training for the three datasets, with respect to the complementary baseline results. That is, for WEBEmo, we compare the joint training (EmotionROI, EmoSet and WEBEmo) with the complementary results of EmotionROI and EmoSet combined. This showcases even more the Few-shot importance of our approach.

Dataset	Size (%)	Performance Impact
EmotionROI	0.45	+7.87% / +7.75%
EmoSet	30.50	+16.58% / +16.37%
WEBEmo	69.05	+6.18% / +3.62%

TABLE IX. Performance impact each dataset individually has on the joint training regime. The performance impact is presented as the difference in Total Accuracy and Zero-shot Accuracy metrics between the joint training and the complementary baseline results.

**APPENDIX C**  
**FULL LIST OF EMOTION SYNONYMS USED FOR DATA AUGMENTATION**

This appendix provides the complete list of synonyms used in our pseudo-label augmentation approach, as described in Section IV-C. For each of the 25 original WEBEmo [14] sentiment labels, we present three additional synonyms. These synonyms were used to expand our emotion vocabulary during training.

Table X lists each original sentiment label with its three synonyms. This expanded set of labels was used in our training process with a 50% chance of random replacement, as detailed in the main text.

WEBEmo [14] sentiment labels	Synonym #1	Synonym #2	Synonym #3
Affection	Love	Fondness	Tenderness
Cheerfulness	Happiness	Joy	Gladness
Confusion	Perplexity	Bewilderment	Puzzlement
Contentment	Satisfaction	Fulfillment	Serenity
Disappointment	Letdown	Frustration	Regret
Disgust	Revulsion	Loathing	Aversion
Enthrallment	Fascination	Enchantment	Allurement
Envy	Jealousy	Resentment	Covetousness
Exasperation	Irritation	Aggravation	Annoyance
Gratitude	Thankfulness	Appreciation	Recognition
Horror	Terror	Dread	Fear
Irritability	Grumpiness	Testiness	Edginess
Lust	Desire	Passion	Love
Neglect	Abandonment	Disregard	Negligence
Nervousness	Anxiety	Tension	Apprehension
Optimism	Hopefulness	Confidence	Positivity
Pride	Self-esteem	Dignity	Vanity
Rage	Fury	Wrath	Outrage
Relief	Comfort	Ease	Reassurance
Sadness	Sorrow	Grief	Despair
Shame	Embarrassment	Humiliation	Guilt
Suffering	Pain	Distress	Agony
Surprise	Astonishment	Amazement	Startlement
Sympathy	Compassion	Empathy	Understanding
Zest	Enthusiasm	Energy	Vigor

TABLE X. WEBEmo sentiment labels and their corresponding synonyms used for pseudo-label augmentation.

Note: The synonyms were originally taken from Bustos *et al.* [35], who used a set of 5 synonyms per label. We reduced this list to 3 synonyms per label using GPT-4 [80].

## APPENDIX D

### COMPARISON OF EMOTIONAL REASONING ON GENERIC TASKS

In this appendix, we provide a detailed comparison of how our LLaVA fine-tuned model with TinyEmo Instruct performs on generic image captioning tasks compared to the baseline LLaVA model. This comparison illustrates the extent to which emotional reasoning capabilities have been integrated into the model knowledge.

Figure 18 shows the outputs of both models when given a simple image captioning prompt for an image of a hand's shadow. The baseline model provides a straightforward, objective description, while the LLaVA fine-tuned model with TinyEmo Instruct incorporates emotional interpretation into its caption.

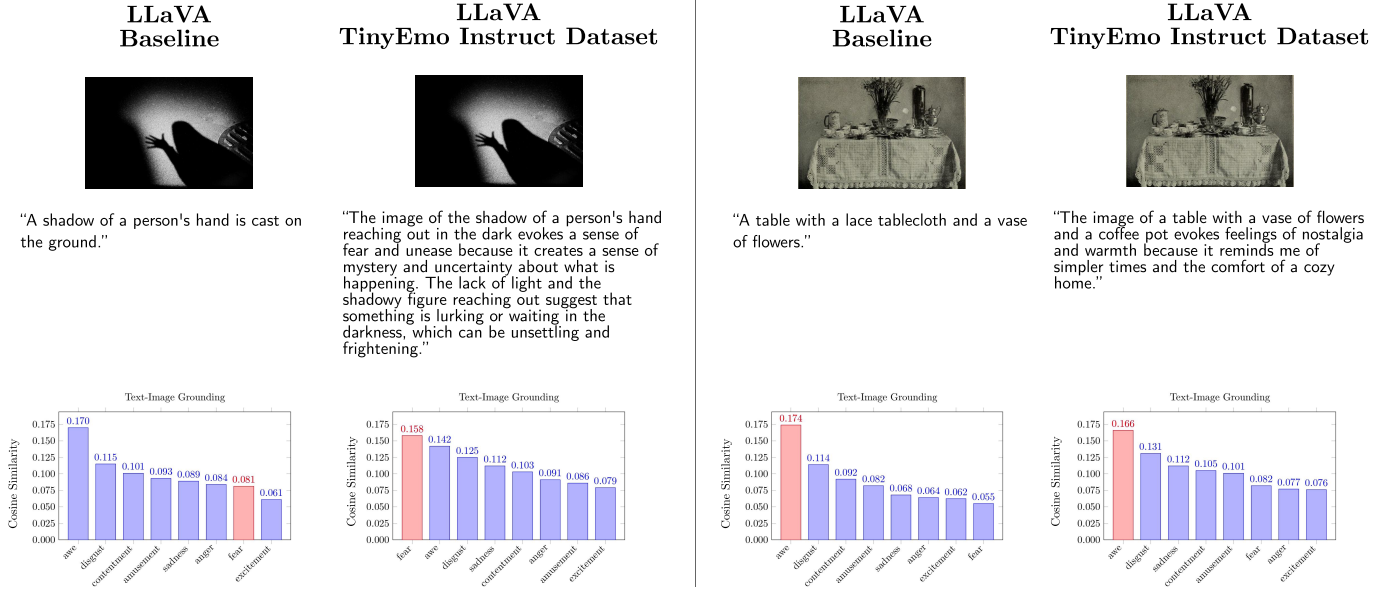


Fig. 16. Comparison of emotional reasoning for a zero-shot sample image of Emotion6 by LLaVA v1.5 7B baseline and LLaVA fine-tuned model with TinyEmo Instruct. We use a general image captioning prompt: "Generate an image caption." to showcase the overfitting of LoRA for the downstream task.

As seen in the figure, the TinyEmo Instruct model not only describes the visual elements but also infers potential emotional responses to the scene. This demonstrates how the model has become more emotionally aware across various prompts, even when not explicitly asked for emotional content.

## APPENDIX E

### INTERESTING NEURONS

#### A. Ablation Study of Individual Neurons

In our investigation of individual neurons, we qualitatively evaluate how each individual neuron in our projector influences the overall performance in image classification tasks. To achieve this, we performed a series of ablation studies in which we iteratively shut down a neuron by setting its activation to zero. We then compute the accuracy on the UnbiasedEmo dataset.

Figure 17 shows the accuracy differences of each ablation with respect the baseline accuracy. The difference are notoriously small, showcasing how individual neurons tend to work in conjunction with the rest of the neural network, and exhibit properties present on fault-tolerant systems. This means that even when a neuron is shut down, other neurons compensate for that, maintaining overall performance.

#### B. Best Neurons at detecting Objects and Emotions

To identify the most influential neurons for detecting specific objects and sentiments, we measured each neuron ability to detect a given object or sentiment by calculating the percentage of top 50 activations associated with that class. For each category, we identified the neuron with the highest detection rate, some of which show interesting causalities.

If we inspect the best neurons for detecting sentiments, more interesting patterns between image classes and sentiment labels emerge.

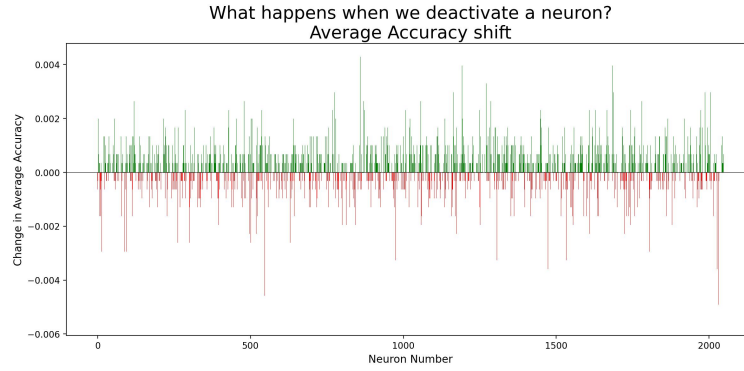


Fig. 17. Ablation study showing the impact of individual neuron deactivation on the final accuracy. Each bar represents the accuracy difference when deactivating a single neuron while all others remain active, compared to the baseline case where all neurons are activated. The x-axis represents individual neuron numbers, and the y-axis shows the change in accuracy.



Fig. 18. Top-left: Neuron 1848 is best at detecting scenery, activating for this feature in 78.00% of its top 50 activations. Top-right: Neuron 1839 is best at detecting teacher, with a detection rate of 36.00% among its top 50 activations. Notably, this neuron also shows a mixture of activations related to teachers and babies, which reflects a reasonable association in context. Bottom-left: Neuron 766 is best at detecting cat, identifying this feature in 46.00% of its top 50 activations. Bottom-right: Neuron 1100 is best at detecting park, with 50.00% of its top 50 activations associated with this scene.

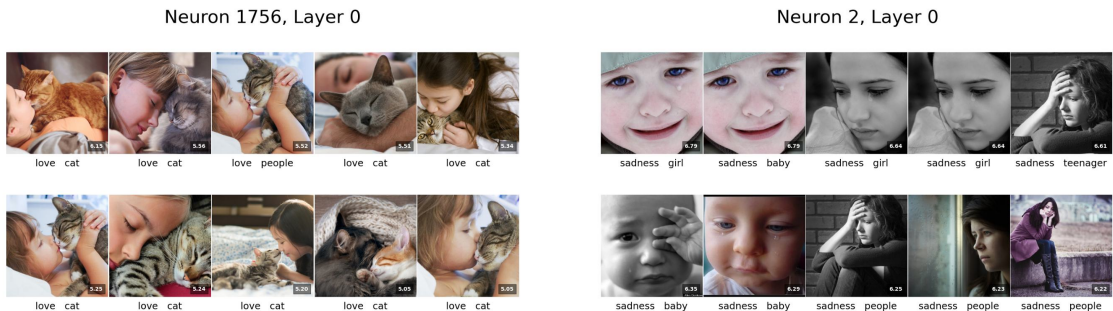


Fig. 19. Left: Neuron 1756, Layer 0 is dedicated to detecting the sentiment of “love” capturing 98% of its top activations. Right: Neuron 2, Layer 0 is specialized in detecting “sadness,” capturing 100% of its top activations.

Figure 19 illustrate the behavior of highly specialized neurons within the network. Left: the “love” neuron (Neuron 1756, Layer

0) with 98% of its top activations corresponding to images labeled with the sentiment “love.” All of the maximal activations feature images of cats cuddling with people, indicating a specialized role in detecting scenes that combine the concepts of love and cats. Right: the “sadness” neuron (Neuron 2, Layer 0), equally specialized, as it detects the “sadness” sentiment in 100% of its top 50 activations. These examples showcase how specific neurons within the network can develop strong specializations for detecting certain sentiments or objects in the dataset.

### C. Cats and Infants Neuron

Neuron 1604’s top 10 activations predominantly featured images of babies and cats. Upon closer inspection, we noticed a common characteristic across these images: open mouths. This observation led us to hypothesize that the neuron might be particularly responsive to this specific facial feature.

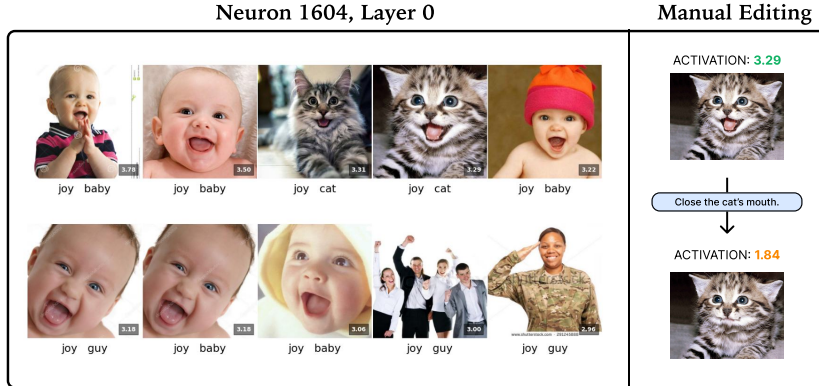


Fig. 20. Neuron 1604 (Layer 0) activation analysis and counterfactual experiment. Left: Top 10 activating images from UnbiasedEmo dataset, showing smiling babies and cats expressing *joy*, with all subjects showing open mouths. Right: Counterfactual experiment using manual editing, with decreased activation (from 3.29 to 1.84) when closing the cat’s mouth, indicating a potential feature affecting the neuron response.

To test our hypothesis, we employed a counterfactual approach as described in Section V-C, manually editing an image of a cat. By closing the cat’s mouth, we observed the neuron’s activation drop significantly from 3.29 to 1.84. This decrease confirms that the open mouth is indeed a feature, although not the only one influencing the neuron.

### ACKNOWLEDGMENT

This work has been partially supported by a UOC grant to AL.

## REFERENCES

- [1] B. Liu, *Sentiment Analysis and Opinion Mining*, ser. Synthesis digital library of engineering and computer science. Morgan & Claypool, 2012. 1
- [2] Paul Ekman, "Facial expressions of emotion: New findings, new questions," *Psychological Science*, vol. 3, pp. 34 – 38, 1992. 1, 2, 8
- [3] W.G. Parrott, *Emotions in Social Psychology: Essential Readings*, ser. Key readings in social psychology. Psychology Press, 2001. 1, 2, 5, 8
- [4] Pj Lang, "International affective picture system (iaps) : affective ratings of pictures and instruction manual," *CTIT technical reports series*, 2005. 1
- [5] Sitara Afzal, Haseeb Ali Khan, Md Jalil Piran, and Jong Weon Lee, "A comprehensive survey on affective computing; challenges, trends, applications, and future directions," *IEEE Access*, 2024. 1
- [6] Duzhen Zhang, Yahan Yu, Chenxing Li, Jiahua Dong, Dan Su, Chenhui Chu, and Dong Yu, "Mm-llms: Recent advances in multimodal large language models," *arXiv preprint arXiv:2401.13601*, 2024. 1, 3
- [7] Wenliang Dai, Junnan Li, Dongxu Li, Anthony Tiong, Junqi Zhao, Weisheng Wang, Boyang Li, Pascale N Fung, and Steven Hoi, "Instructblip: Towards general-purpose vision-language models with instruction tuning," in *Advances in Neural Information Processing Systems*, vol. 36, 2023, pp. 49 250–49 267. 1, 3, 14
- [8] Haotian Liu, Chunyuan Li, Qingyang Wu, and Yong Jae Lee, "Visual instruction tuning," *Advances in neural information processing systems*, vol. 36, 2024. 1, 3, 5, 14
- [9] Dosovitskiy Alexey, "An image is worth 16x16 words: Transformers for image recognition at scale," *arXiv preprint arXiv: 2010.11929*, 2020. 1
- [10] Hongxia Xie, Chu-Jun Peng, Yu-Wen Tseng, Hung-Jen Chen, Chan-Feng Hsu, Hong-Han Shuai, and Wen-Huang Cheng, "Emovit: Revolutionizing emotion insights with visual instruction tuning," in *Proceedings of the IEEE/CVF Conference on Computer Vision and Pattern Recognition*, 2024, pp. 26 596–26 605. 1, 2, 3, 8, 14, 16
- [11] Sicheng Zhao, Xingxu Yao, Jufeng Yang, Guoli Jia, Guiguang Ding, Tat-Seng Chua, Björn W. Schuller, and Kurt Keutzer, "Affective image content analysis: Two decades review and new perspectives," *IEEE Transactions on Pattern Analysis and Machine Intelligence*, vol. 44, no. 10, pp. 6729–6751, 2022. 1
- [12] Yuhui Zhang, Alyssa Unell, Xiaohan Wang, Dhruba Ghosh, Yuchang Su, Ludwig Schmidt, and Serena Yeung-Levy, "Why are visually-grounded language models bad at image classification?" *arXiv preprint arXiv:2405.18415*, 2024. 2
- [13] Gregor Geigle, Radu Timofte, and Goran Glavaš, "African or european swallow? benchmarking large vision-language models for fine-grained object classification," *arXiv preprint arXiv:2406.14496*, 2024. 2, 3, 5, 8
- [14] Rameswar Panda, Jianming Zhang, Haoxiang Li, Joon-Young Lee, Xin Lu, and Amit K Roy-Chowdhury, "Contemplating visual emotions: Understanding and overcoming dataset bias," in *Proceedings of the European Conference on Computer Vision (ECCV)*, 2018, pp. 579–595. 2, 5, 8, 14, 22
- [15] Jingyuan Yang, Qirui Huang, Tingting Ding, Dani Lischinski, Danny Cohen-Or, and Hui Huang, "Emoset: A large-scale visual emotion dataset with rich attributes," in *Proceedings of the IEEE/CVF International Conference on Computer Vision*, 2023, pp. 20 383–20 394. 2, 3, 8, 14
- [16] Marie Katsurai and Shin'ichi Satoh, "Image sentiment analysis using latent correlations among visual, textual, and sentiment views," in *2016 IEEE International Conference on Acoustics, Speech and Signal Processing (ICASSP)*, 2016, pp. 2837–2841. 2
- [17] Quanzeng You, Jiebo Luo, Hailin Jin, and Jianchao Yang, "Building a large scale dataset for image emotion recognition: The fine print and the benchmark," in *Proceedings of the AAAI conference on artificial intelligence*, vol. 30, no. 1, 2016. 2, 8
- [18] Jana Machajdik and Allan Hanbury, "Affective image classification using features inspired by psychology and art theory," in *Proceedings of the 18th ACM international conference on Multimedia*, 2010, pp. 83–92. 2, 8
- [19] Peter J Lang, Margaret M Bradley, Bruce N Cuthbert *et al.*, "International affective picture system (iaps): Instruction manual and affective ratings," *The center for research in psychophysiology, University of Florida*, 1999. 2
- [20] Runjia Li, Shuyang Sun, Mohamed Elhoseiny, and Philip Torr, "Oxfordtvg-hic: Can machine make humorous captions from images?" in *Proceedings of the IEEE/CVF International Conference on Computer Vision*, 2023, pp. 20 293–20 303. 2
- [21] Ronak Kosti, Jose M Alvarez, Adria Recasens, and Agata Lapedriza, "Context based emotion recognition using emotic dataset," *IEEE transactions on pattern analysis and machine intelligence*, vol. 42, no. 11, pp. 2755–2766, 2019. 2
- [22] Ronak Kosti, Jose M. Alvarez, Adria Recasens, and Agata Lapedriza, "Emotion recognition in context," in *2017 IEEE Conference on Computer Vision and Pattern Recognition (CVPR)*, 2017, pp. 1960–1968. 2
- [23] Kuan-Chuan Peng, Amir Sadovnik, Andrew Gallagher, and Tsuhan Chen, "Where do emotions come from? predicting the emotion stimuli map," in *2016 IEEE International Conference on Image Processing (ICIP)*, 2016, pp. 614–618. 2, 8, 14
- [24] Rina carines Cabral, Soyeon caren Han, Josiah Poon, and Goran Nenadic, "Mm-emog: Multi-label emotion graph representation for mental health classification on social media," *robotics*, vol. 13, no. 3, p. 53, Mar. 2024. 2
- [25] Panos Achlioptas, Maks Ovsjanikov, Kilichbek Haydarov, Mohamed Elhoseiny, and Leonidas J Guibas, "Artemis: Affective language for visual art," in *Proceedings of the IEEE/CVF Conference on Computer Vision and Pattern Recognition*, 2021, pp. 11 569–11 579. 2
- [26] Panos Achlioptas, Maks Ovsjanikov, Leonidas Guibas, and Sergey Tulyakov, "Affection: Learning affective explanations for real-world visual data," in *Proceedings of the IEEE/CVF Conference on Computer Vision and Pattern Recognition*, 2023, pp. 6641–6651. 2, 12
- [27] Tsung-Yi Lin, Michael Maire, Serge Belongie, James Hays, Pietro Perona, Deva Ramanan, Piotr Dollár, and C Lawrence Zitnick, "Microsoft coco: Common objects in context," in *Computer Vision–ECCV 2014: 13th European Conference, Zurich, Switzerland, September 6–12, 2014, Proceedings, Part V 13*. Springer, 2014, pp. 740–755. 2
- [28] Yoshua Bengio, Jérôme Louradour, Ronan Collobert, and Jason Weston, "Curriculum learning," in *Proceedings of the 26th Annual International Conference on Machine Learning*, ser. ICML '09. New York, NY, USA: Association for Computing Machinery, 2009, p. 41–48. 2
- [29] Ashish Vaswani, Noam Shazeer, Niki Parmar, Jakob Uszkoreit, Llion Jones, Aidan N. Gomez, Łukasz Kaiser, and Illia Polosukhin, "Attention is all you need," 2023. 3
- [30] Jacob Devlin, Ming-Wei Chang, Kenton Lee, and Kristina Toutanova, "Bert: Pre-training of deep bidirectional transformers for language understanding," 2019. 3
- [31] Brandon McKinzie, Zhe Gan, Jean-Philippe Fauconnier, Sam Dodge, Bowen Zhang, Philipp Dufter, Dhruti Shah, Xianzhi Du, Futang Peng, Floris Weers *et al.*, "Mm1: Methods, analysis & insights from multimodal llm pre-training," 2024. 3, 7
- [32] Alec Radford, Jong Wook Kim, Chris Hallacy, Aditya Ramesh, Gabriel Goh, Sandhini Agarwal, Girish Sastry, Amanda Askell, Pamela Mishkin, Jack Clark *et al.*, "Learning transferable visual models from natural language supervision," 2021. 3, 6, 7, 14
- [33] Brandon McKinzie, Zhe Gan, Jean-Philippe Fauconnier, Sam Dodge, Bowen Zhang, Philipp Dufter, Dhruti Shah, Xianzhi Du, Futang Peng, Floris Weers *et al.*, "Mm1: Methods, analysis & insights from multimodal llm pre-training," 2024. 3, 10
- [34] Maxime Oquab, Timothée Darcret, Théo Moutakanni, Huy Vo, Marc Szafraniec, Vasil Khalidov, Pierre Fernandez, Daniel Haziza, Francisco Massa, Alaaeldin El-Nouby *et al.*, "Dinov2: Learning robust visual features without supervision," 2024. 3
- [35] Cristina Bustos, Carles Civit, Brian Du, Albert Solé-Ribalta, and Agata Lapedriza, "On the use of vision-language models for visual sentiment analysis: a study on clip," in *2023 11th International Conference on Affective Computing and Intelligent Interaction (ACII)*. IEEE, 2023, pp. 1–8. 3, 10, 14, 22
- [36] Jason Wei, Maarten Bosma, Vincent Zhao, Kelvin Guu, Adams Wei Yu, Brian Lester, Nan Du, Andrew M. Dai, and Quoc V Le, "Finetuned language models are zero-shot learners," in *International Conference on Learning Representations*, 2022. 3
- [37] Long Ouyang, Jeffrey Wu, Xu Jiang, Diogo Almeida, Carroll Wainwright, Pamela Mishkin, Chong Zhang, Sandhini Agarwal, Katarina Slama, Alex Ray *et al.*, "Training language models to follow instructions with human feedback," *Advances in neural information processing systems*, vol. 35, pp. 27 730–27 744, 2022. 3

[38] Haotian Liu, Chunyuan Li, Yuheng Li, and Yong Jae Lee, "Improved baselines with visual instruction tuning," in *Proceedings of the IEEE/CVF Conference on Computer Vision and Pattern Recognition*, 2024, pp. 26296–26306. 3, 7, 8

[39] Yang Zhao, Zhipie Lin, Daquan Zhou, Zilong Huang, Jashi Feng, and Bingyi Kang, "Bubogpt: Enabling visual grounding in multi-modal llms," 2023. 3

[40] Junnan Li, Dongxu Li, Silvio Savarese, and Steven Hoi, "Blip-2: Bootstrapping language-image pre-training with frozen image encoders and large language models," 2023. 3, 14

[41] Junbum Cha, Wooyoung Kang, Jonghwan Mun, and Byungseok Roh, "Honeybee: Locality-enhanced projector for multimodal llm," 2024. 3

[42] Kaiming He, Xiangyu Zhang, Shaoqing Ren, and Jian Sun, "Deep residual learning for image recognition," 2015. 3

[43] Dongxu Li, Junnan Li, Hung Le, Guangsen Wang, Silvio Savarese, and Steven C.H. Hoi, "LAVIS: A one-stop library for language-vision intelligence," in *Proceedings of the 61st Annual Meeting of the Association for Computational Linguistics (Volume 3: System Demonstrations)*. Association for Computational Linguistics, 2023, pp. 31–41. 3

[44] Meta AI, "Introducing llama 3.1: Our most capable models to date," <https://ai.meta.com/blog/meta-llama-3-1/>, July 2024, accessed: 2024-08-03. 3

[45] Geoffrey Hinton, "Distilling the knowledge in a neural network," *arXiv preprint arXiv:1503.02531*, 2015. 3

[46] Geoffrey Hinton, Oriol Vinyals, and Jeff Dean, "Dark knowledge," *Presented as the keynote in BayLearn*, vol. 2, no. 2, 2014. 4

[47] Yoon Kim and Alexander M Rush, "Sequence-level knowledge distillation," *arXiv preprint arXiv:1606.07947*, 2016. 4

[48] Abhimanyu Dubey, Abhinav Jauhri, Abhinav Pandey, Abhishek Kadian, Ahmad Al-Dahle, Aiesha Letman, Akhil Mathur, Alan Schelten, Amy Yang, Angela Fan *et al.*, "The llama 3 herd of models," *arXiv preprint arXiv:2407.21783*, 2024. 4

[49] Suriya Gunasekar, Yi Zhang, Jyoti Aneja, Caio César Teodoro Mendes, Allie Del Giorno, Sivakanth Gopi, Mojan Javaheripi, Piero Kauffmann, Gustavo de Rosa, Olli Saarikivi *et al.*, "Textbooks are all you need," *arXiv preprint arXiv:2306.11644*, 2023. 4, 5, 14

[50] Afra Alishahi, Grzegorz Chrupała, and Tal Linzen, "Analyzing and interpreting neural networks for nlp: A report on the first blackboxnlp workshop," *Natural Language Engineering*, vol. 25, no. 4, pp. 543–557, 2019. 4

[51] Haoyan Luo and Lucia Specia, "From understanding to utilization: A survey on explainability for large language models," *arXiv preprint arXiv:2401.12874*, 2024. 4

[52] Kevin Ro Wang, Alexandre Variengien, Arthur Conmy, Buck Shlegeris, and Jacob Steinhardt, "Interpretability in the wild: a circuit for indirect object identification in GPT-2 small," in *The Eleventh International Conference on Learning Representations*, 2023. 4

[53] Chris Olah, "Mechanistic interpretability, variables, and the importance of interpretable bases," <https://www.transformer-circuits.pub/2022/mech-interp-essay>, 2022, accessed: 2024-07-13. 4

[54] Chandan Singh, Jeevana Priya Inala, Michel Galley, Rich Caruana, and Jianfeng Gao, "Rethinking interpretability in the era of large language models," *arXiv preprint arXiv:2402.01761*, 2024. 4

[55] Laura Weidinger, John Mellor, Maribeth Rauh, Conor Griffin, Jonathan Uesato, Po-Sen Huang, Myra Cheng, Mia Glaese, Borja Balle, Atoosa Kasirzadeh *et al.*, "Ethical and social risks of harm from language models," *arXiv preprint arXiv:2112.04359*, 2021. 4

[56] Jitang Li and Jinzheng Li, "Memory, consciousness and large language model," *arXiv preprint arXiv:2401.02509*, 2024. 4

[57] David Bau, Bolei Zhou, Aditya Khosla, Aude Oliva, and Antonio Torralba, "Network dissection: Quantifying interpretability of deep visual representations," in *Proceedings of the IEEE conference on computer vision and pattern recognition*, 2017, pp. 6541–6549. 4

[58] David Bau, Jun-Yan Zhu, Hendrik Strobelt, Agata Lapedriza, Bolei Zhou, and Antonio Torralba, "Understanding the role of individual units in a deep neural network," *Proceedings of the National Academy of Sciences*, vol. 117, no. 48, pp. 30071–30078, 2020. 4

[59] Tamar Rott Shaham, Sarah Schwettmann, Franklin Wang, Achyuta Rajaram, Evan Hernandez, Jacob Andreas, and Antonio Torralba, "A multimodal automated interpretability agent," in *Forty-first International Conference on Machine Learning*, 2024. 4, 18

[60] Muyang He, Yixin Liu, Boya Wu, Jianhao Yuan, Yueze Wang, Tiejun Huang, and Bo Zhao, "Efficient multimodal learning from data-centric perspective," *arXiv preprint arXiv:2402.11530*, 2024. 4, 5, 21

[61] Xiaohua Zhai, Basil Mustafa, Alexander Kolesnikov, and Lucas Beyer, "Sigmoid loss for language image pre-training," in *Proceedings of the IEEE/CVF International Conference on Computer Vision*, 2023, pp. 11975–11986. 5, 7

[62] Yuanzhi Li, Sébastien Bubeck, Ronen Eldan, Allie Del Giorno, Suriya Gunasekar, and Yin Tat Lee, "Textbooks are all you need ii: phi-1.5 technical report," *arXiv preprint arXiv:2309.05463*, 2023. 5

[63] Chaoyou Fu, Peixian Chen, Yunhang Shen, Yulei Qin, Mengdan Zhang, Xu Lin, Jinrui Yang, Xiawu Zheng, Ke Li, Xing Sun *et al.*, "Mme: A comprehensive evaluation benchmark for multimodal large language models," *arXiv preprint arXiv:2306.13394*, 2023. 5

[64] Wei-Lin Chiang, Lianmin Zheng, Ying Sheng, Anastasios Nikolas Angelopoulos, Tianle Li, Dacheng Li, Hao Zhang, Banghua Zhu, Michael Jordan, Joseph E Gonzalez *et al.*, "Chatbot arena: An open platform for evaluating llms by human preference," *arXiv preprint arXiv:2403.04132*, 2024. 5

[65] Dan Hendrycks and Kevin Gimpel, "Gaussian error linear units (gelus)," *arXiv preprint arXiv:1606.08415*, 2016. 6

[66] Lucas Beyer, Andreas Steiner, André Susano Pinto, Alexander Kolesnikov, Xiao Wang, Daniel Salz, Maxim Neumann, Ibrahim Alabdulmohsin, Michael Tschanen, Emanuele Bugliarello *et al.*, "Paligemma: A versatile 3b vlm for transfer," *arXiv preprint arXiv:2407.07726*, 2024. 6, 7

[67] Niklas Muennighoff, Nouamane Tazi, Loïc Magne, and Nils Reimers, "Mteb: Massive text embedding benchmark," *arXiv preprint arXiv:2210.07316*, 2022. 6, 7

[68] Kihyuk Sohn, "Improved deep metric learning with multi-class n-pair loss objective," in *Advances in Neural Information Processing Systems*, D. Lee, M. Sugiyama, U. Luxburg, I. Guyon, and R. Garnett, Eds., vol. 29, 2016. 6

[69] Junlong Jia, Ying Hu, Xi Weng, Yiming Shi, Miao Li, Xingjian Zhang, Baichuan Zhou, Ziyu Liu, Jie Luo, Lei Huang *et al.*, "Tinnyllava factory: A modularized codebase for small-scale large multimodal models," *arXiv preprint arXiv:2405.11788*, 2024. 7

[70] Baichuan Zhou, Ying Hu, Xi Weng, Junlong Jia, Jie Luo, Xien Liu, Ji Wu, and Lei Huang, "Tinnyllava: A framework of small-scale large multimodal models," 2024. 7

[71] Maxime Oquab, Timothée Darcret, Théo Moutakanni, Huy Vo, Marc Szafraniec, Vasil Khalidov, Pierre Fernandez, Daniel Haziza, Francisco Massa, Alaeldin El-Nouby *et al.*, "Dinov2: Learning robust visual features without supervision," *arXiv preprint arXiv:2304.07193*, 2023. 7

[72] Sachin Mehta, Mohammad Hosseini Sekhavat, Qingqing Cao, Maxwell Horton, Yanzi Jin, Chenfan Sun, Seyed Iman Mirzadeh, Mahyar Najibi, Dmitry Belenko, Peter Zatloukal *et al.*, "Openelm: An efficient language model family with open training and inference framework," in *Workshop on Efficient Systems for Foundation Models II@ ICML2024*, 2024. 7, 14

[73] Peiyuan Zhang, Guangtao Zeng, Tianduo Wang, and Wei Lu, "Tinnyllama: An open-source small language model," 2024. 7, 14

[74] Guilherme Penedo, Quentin Malartic, Daniel Hesslow, Ruxandra Cojocaru, Alessandro Cappelli, Hamza Alobaidli, Baptiste Pannier, Ebtesam Almazrouei, and Julien Launay, "The refinedweb dataset for falcon llm: outperforming curated corpora with web data, and web data only," *arXiv preprint arXiv:2306.01116*, 2023. 7

[75] Leo Gao, Stella Biderman, Sid Black, Laurence Golding, Travis Hoppe, Charles Foster, Jason Phang, Horace He, Anish Thite, Noa Nabeshima *et al.*, "The pile: An 800gb dataset of diverse text for language modeling," *arXiv preprint arXiv:2101.00027*, 2020. 7

[76] Together Computer, "Redpajama: An open source recipe to reproduce llama training dataset," 2023. [Online]. Available: <https://github.com/togethercomputer/RedPajama-Data> 7

[77] Luca Soldaini, Rodney Kinney, Akshita Bhagia, Dustin Schwenk, David Atkinson, Russell Arthur, Ben Bogin, Khyathi Chandu, Jennifer Dumas, Yanai Elazar *et al.*, "Dolma: An open corpus of three trillion tokens for language model pretraining research," *arXiv preprint arXiv:2402.00159*, 2024. 7

[78] Daria Soboleva, Faisal Al-Khateeb, Robert Myers, Jacob R Steeves, Joel Hestness, and Nolan Dey, "SlimPajama: A 627B token cleaned and deduplicated version of RedPajama," <https://www.cerebras.net/blog/slimpajama-a-627b-token-cleaned-and-deduplicated-version-of-redpajama>, 2023. [Online]. Available: <https://huggingface.co/datasets/cerebras/SlimPajama-627B> 7

- [79] Raymond Li, Loubna Ben Allal, Yangtian Zi, Niklas Muennighoff, Denis Kocetkov, Chenghao Mou, Marc Marone, Christopher Akiki, Jia Li, Jenny Chim *et al.*, “Starcoder: may the source be with you!” *arXiv preprint arXiv:2305.06161*, 2023. [7](#)
- [80] Josh Achiam, Steven Adler, Sandhini Agarwal, Lama Ahmad, Ilge Akkaya, Florencia Leoni Aleman, Diogo Almeida, Janko Altenschmidt, Sam Altman, Shyamal Anadkat *et al.*, “Gpt-4 technical report,” *arXiv preprint arXiv:2303.08774*, 2023. [7](#), [22](#)
- [81] Joseph A. Mikels, Barbara L. Fredrickson, Gregory R. Larkin, Casey M. Lindberg, Sam J. Maglio, and Patricia A. Reuter-Lorenz, “Emotional category data on images from the international affective picture system,” *Behavior Research Methods*, vol. 37, no. 4, pp. 626–630, 2005. [8](#)
- [82] Jean-Baptiste Alayrac, Jeff Donahue, Pauline Luc, Antoine Miech, Iain Barr, Yana Hasson, Karel Lenc, Arthur Mensch, Katherine Millican, Malcolm Reynolds *et al.*, “Flamingo: a visual language model for few-shot learning,” *Advances in neural information processing systems*, vol. 35, pp. 23 716–23 736, 2022. [14](#)
- [83] Guoli Jia and Jufeng Yang, “S2-ver: Semi-supervised visual emotion recognition,” in *ECCV*, 2022. [14](#)
- [84] Jason Wei, Xuezhi Wang, Dale Schuurmans, Maarten Bosma, Fei Xia, Ed Chi, Quoc V Le, Denny Zhou *et al.*, “Chain-of-thought prompting elicits reasoning in large language models,” *Advances in neural information processing systems*, vol. 35, pp. 24 824–24 837, 2022. [16](#)
- [85] Phillip Howard, Anahita Bhivandiwalla, Kathleen C Fraser, and Svetlana Kiritchenko, “Uncovering bias in large vision-language models with counterfactuals,” *arXiv preprint arXiv:2404.00166*, 2024. [18](#)
- [86] Phillip Isola, Jun-Yan Zhu, Tinghui Zhou, and Alexei A Efros, “Image-to-image translation with conditional adversarial networks,” in *Proceedings of the IEEE conference on computer vision and pattern recognition*, 2017, pp. 1125–1134. [18](#)
- [87] Aditya Ramesh, Mikhail Pavlov, Gabriel Goh, Scott Gray, Chelsea Voss, Alec Radford, Mark Chen, and Ilya Sutskever, “Zero-shot text-to-image generation,” in *International conference on machine learning*. Pmlr, 2021, pp. 8821–8831. [18](#)